REPORT DOCUMENTATION PAGE

Form Approved OMB No. 0704-0188

1. REPORT DATE *(DD-MM-YYYY)*	2. REPORT TYPE	3. DATES COVERED *(From – To)*
02-07-2004	Final Report	01-Mar-02 - 19-Aug-04

4. TITLE AND SUBTITLE

Photo Electron Paramagnetic Resonance (Photo EPR) Study Of Trapping And Recombination Processes In Semi-Insulating 4H, 6H Sic Crystals Over A Wide Temperature Interval

5a. CONTRACT NUMBER
STCU Registration No: P-092

5b. GRANT NUMBER

5c. PROGRAM ELEMENT NUMBER

6. AUTHOR(S)

Dr. Ekaterina Kalabukhova

5d. PROJECT NUMBER

5d. TASK NUMBER

5e. WORK UNIT NUMBER

7. PERFORMING ORGANIZATION NAME(S) AND ADDRESS(ES)

National Academy of Sciences of the Ukraine
Pr. Nauki, 45
Kiev 252028
Ukraine

8. PERFORMING ORGANIZATION REPORT NUMBER

N/A

9. SPONSORING/MONITORING AGENCY NAME(S) AND ADDRESS(ES)

EOARD
PSC 802 BOX 14
FPO 09499-0014

10. SPONSOR/MONITOR'S ACRONYM(S)

11. SPONSOR/MONITOR'S REPORT NUMBER(S)
STCU 01-8006

12. DISTRIBUTION/AVAILABILITY STATEMENT

Approved for public release; distribution is unlimited.

13. SUPPLEMENTARY NOTES

14. ABSTRACT

This report results from a contract tasking National Academy of Sciences of the Ukraine as follows: The objective of this project is to clarify the physics and materials science of a material with great industrial potential, as a substrate used in a wide variety of electronic and optical devices. The Institute for Semiconductor Physics, with more than 15 years of experience in semiconductor material analysis, is uniquely qualified to conduct this research and has developed unique experimental facilties to carry our this investigation.

15. SUBJECT TERMS
EOARD, Physics, Solid State Physics

16. SECURITY CLASSIFICATION OF:			17. LIMITATION OF ABSTRACT	18, NUMBER OF PAGES	19a. NAME OF RESPONSIBLE PERSON
a. REPORT	b. ABSTRACT	c. THIS PAGE			DONALD J SMITH
UNCLAS	UNCLAS	UNCLAS	UL	47	19b. TELEPHONE NUMBER *(Include area code)* +44 (0)20 7514 4953

Project main idea

Semi-insulating (s.-i.) silicon carbide is required for a variety of applications including microwave field effect transistors and other devices intended for the high power or high temperature applications. The unique properties of this material make it particularly attractive for both SiC and GaN based devices. Although considerable progress has been made in the technology of s.-i. SiC material, semi-insulating SiC is available commercially at prohibitive prices and in limited quantities. One reason for the low yield and high cost is the fact that the nature of the dominant deep levels responsible for the semi-insulating properties of the SiC material are not known and so growth processes can not be adjusted to optimize the concentration of this defect. This project directly addresses that problem.

Mostly the s.-i. material is produced by doping the silicon carbide with vanadium which results in the compensation of residual acceptors or donors and produces material that is nearly insulating at room temperature. Vanadium substitutes for silicon in SiC and is amphoteric, producing either a donor or acceptor level depending on the position of the Fermi level. The donor level, located near midgap, is preferred for s.-i. material that will keep its high resistance at elevated temperature.

However, it has recently been shown that, in addition to vanadium, another deep levels due to intrinsic defects can pin the Fermi level in s.-i. SiC [1]. The deep intrinsic defects which have energies of 1 eV or more have been reported by many authors. But usually they have been studied in conducting or irradiated material. The intrinsic defect with energy level at EC - 1.1 eV has been detected by ODMR in conducting 6H SiC and is postulated as the dominant lifetime limiting defect in both the bulk and epitaxial material [2]. The DLTS measurements of electron irradiated 4H epitaxial material indicated numerous deep levels from 0.45 to 1.65 eV [3,4]. The level at E_C - 1.65 eV was observed in unirradiated material but enhanced by radiation. The level at E_C - 1.13 eV was observed only after higher dose irradiations. The energy levels at 1.18 eV and 1.73 eV in 4H material and at 1.07 and 1.59 eV in 6H samples have been determined from Optical Admittance Spectroscopy (OAS) experiments on conducting n-type material.

But in spite of progress in experimental data the atomistic identification of the defects is still limited. In this case Electron Paramagnetic Resonance (EPR) is one of the very few techniques which enables to identify the point defects and to determine the local symmetry of their closest environment. At the moment some of the point defects have been conclusively identified from magnetic resonance methods including:
- silicon monovacancy in its singly negative charge state in 6H SiC [5],
- carbon monovacancy in single positive charge state in 4H SiC [6],
- carbon antisite-carbon vacancy pair in 6H SiC [7],
- silicon antisite in single positive charge state in 4H SiC [8].

Recently the photo EPR technique has been used to determine the energy level of the deep defect in s.-i. 4H SiC. But severe overlapping between different EPR spectra appeared in s.-i. material under illumination at 9.75 GHz leads to the incorrect determination of the energy level of the deep defect [9]. At the same time from the high frequency (94 GHz) photo EPR study the energy level of the defect with the same EPR parameters in p-type irradiated 4H SiC has been determined as deep donor level of carbon vacancy in positive charge state at 1.47 eV above the valence band [6]. This fact is also suggest that for obtaining reliable EPR data it is necessary to perform the measurements at high frequency in order to avoid the problem of overlapping between different spectra.

The main idea of the project was to establish the microscopic models of the deep intrinsic defects responsible for semi-insulating (s.-i.) properties of 4H SiC material and electronic model of the trapping and recombination (TR) process of non-equilibrium charge carriers involving deep intrinsic defects by photo EPR methods to be able to adjust and optimize the growth parameters of semi-insulating material.

It is well know that trapping and recombination (TR) of non-equilibrium charge carriers at defects and impurity levels are among the most important processes in semiconductor physics and technology. An understanding of these processes is essential for device development with SiC. Therefore the objective of the present project was to establish the role of deep centers in the trapping and recombination process occurring in semi-insulating SiC.

The project has been undertaken in close collaboration with the Air Force Research Laboratory, Materials and Manufacturing Directorate, AFRL/MLPS, Wright-Patterson Air Force Base, Ohio which is engaged in electrically and optically characterization of SiC material. The correlation between electrical, optical and EPR data has been established.

The results obtained will be used for optimization of the growth parameters that will promote a low cost yield of s.-i. SiC wafers. In particular, to optimize the vapor composition inside the growth cell either SiC-C or SiC-Si type that would provide a stable growth conditions for crystals of considerable size with desired concentration of the intrinsic defects.

Technical approach

In this work the systematic and comprehensive High Field multifrequency EPR study of 4H s.-i. samples has been carried out to identify the intrinsic defects responsible for the s-i. feature of SiC.

Two sets of 4H s.-i. samples were investigated. One set is commercial, undoped HPSI 4H-SiC grown by sublimation vapor transport technique (PVT), while the second set is vanadium doped PVT 4H SiC.

In undoped 4H s.-i. samples grown by the sublimation vapor transport technique vanadium was found to be below the detection limit of secondary ion mass spectrometry (SIMS) equipment ($<10^{15}$ cm^{-3}). Trace amounts of titanium and oxygen were the only impurities detected by SIMS in these samples. Temperature dependent Hall effect measurements showed that the Fermi level was pinned at the $E_C - 1.1$ eV level. Optical admittance spectroscopy measurements, Fig. 1, show only the 1.1 eV level and near band edge response.

The crystals were used of about 10x15 mm^2 size and thickness (~(0.3-0.6)mm that make it possible to measure EPR spectra at different frequencies and in different crystallographic planes. The s.-i. samples have been annealed in the temperature interval from 1400^0C to 1800^0C.

Rapid annealing has been made with a strip heater. It enabled us to perform thermal annealing with heating rate of up to 1500 °C/s and minimal annealing stage duration of 5 s. Thermal annealing has been performed in the He flow. These conditions completely ruled out possibility for epitaxial film formation on the crystal surfaces. The annealing temperature T_{ann} varied from 1400 up to 1800 °C; it was monitored with an optical pyrometer.

The measurements have been performed in the temperature interval from 4.2 K to 140 K in X-, Q-, D-band. EPR spectra have been investigated in the dark. The samples have been measured before annealing and after annealing in the temperature range of $1400\ ^0$C - $1800\ ^0$C.

Photo-EPR measurements including excitation and quenching methods have been taken in digitally controlled Q-band EPR spectrometer equipped with additional optical arrangements. Q-band EPR spectrometer includes frequency tunable 37 GHz microwave resonator providing the possibility to work with samples of different dimensions, geometry to rotate and illuminate the samples in the cavity in the range of 320 - 1000 nm.

Spectra were studied in the temperature interval from 4.2 K to 140 K The specimen was fixed on the end of a quartz rod which was simultaneously used as a light guide and a sample holder in the resonator. The crystal was oriented in such way that the growth axis (**c**-axis) was perpendicular to the magnetic field. Two light sources were used for illuminating the sample. The excitation measurements were performed using a mercury high-pressure vapour lamp (250 W) and a 365 nm interference filter. The sample holder was used as a light guide with a collecting lens to focus the light on the sample. The quenching experiments were performed with a 100 W xenon lamp combined with prismatic monochromator for a wavelength range of 380 nm to 1000 nm or with different interference filters for a wavelength range of 380 nm to 1000 nm. With this arrangement it was possible to obtain continuous quenching spectra.

The effect of annealing temperature, doping level, degree of compensation and influence of stoichiometry have been investigated. This permitted the determination of the nature of the dominant intrinsic defects in intentionally doped with vanadium, manganese and in vanadium free 4H s.-i. samples along with their energy characteristics.

The investigation of the recombination process between photo created electrons and holes and determination of the energy characteristics, charge states of the defects has been performed through the photo-EPR methods including photo-excitation and photo-quenching technique.

The recombination process in the s. - i. 4H-SiC sample has been investigated by means of simple kinetics experiment. Generally at least two photosensitive EPR signals are necessary to make such experiments possible. For this experiment, the EPR signals were first excited to a maximum value with above band–gap light then the exciting light was switched off and the quenching light is switched on. Considering that in s.-i. samples shallow donors and acceptors are not significantly populated prior to illumination, the first step in the experiment was excitation of the sample with UV light which induces the neutralization of the shallow donors and acceptors. After the donors and acceptors have been neutralized, the effects of sub-band gap light can be studied. The spectral dependencies of the photo-quenching processes of the EPR spectra after excitation the sample with above band gap light has been investigated to establish the energy characteristics and mechanism of TR process in s.-i. sample.

Microscopic models for intrinsic defects have been identified on the base of EPR spectrum symmetry, the hyperfine structure due to the interaction with adjacent Si (C) neighbors, and the conditions for EPR spectrum observations including temperature range, level of microwave power, wavelength of excitation.

The proposed microscopic models for intrinsic defects have been compared with the theoretical prediction including the formation energies, ionization levels and local geometries of the relaxed structures for the defects residing hexagonal and cubic lattice site. Experimentally determined ionization levels of intrinsic defects have been discussed in a view of the theoretical predicted levels for the intrinsic defects in different charge and spin states.

It should be notice, that in as-grown SiC sample the intensity of the EPR lines from intrinsic defects usually of one order weaker than that in irradiated SiC. This fact is often hampered EPR identification of the intrinsic defects using their ligand hyperfine structure in the case when the defect resides the silicon site since there is better chance of detecting the hyperfine structure of ^{29}Si (I=1/2, 4.7% natural abundance) than that of ^{13}C (I=1/2, 1.16 % natural abundance).

From the other side, after illumination of the as-grown s.-i. sample with the light, a few intrinsic defects appeared in EPR spectrum along with the EPR spectrum of shallow donor nitrogen and boron acceptor resulting in severe overlapping between different EPR spectra. Therefore the experiment should be performed at high microwave frequency.

In order to avoid these problems the identification of the intrinsic defects observed in s.i. 4H SiC has been undertaken on as-grown 4H SiC samples in which some of the defects are also present but with higher concentrations.

The analysis of the ligand HF structure has been performed through EPR measurements at 140 GHz using the advantages of high-frequency EPR, namely high spectral resolution and enhancement of detection sensitivity.

EPR measurements at 140 GHz were performed in a superheterodyne D-band EPR setup equipped with semi-confocal cavity consisting of a spherical and a flat mirror using as a sample holder and allowing to work with the samples of large size up to 6x6x0.5mm^3.

Technical progress overview

There is a current interest in SiC which has deep levels to produce semi-insulating microwave device substrates. Among the deep levels, the dominant recombination centers (i.e. the life-time-limiting defects), despite their essential importance, are still unknown. One of the suitable experimental techniques which are sensitive to carrier recombination process and can give the detail information about electronic structure of the recombination centers is the photo EPR technique. Also, conclusions about the level positions in the bandgap of the defects and impurities, and on charge, spin state, can be obtained using the photo excitation and photo quenching EPR method.

In this work a systematic and comprehensive photo EPR study of s.-i. 4H SiC has been carried aimed to reveal and identify the defects playing important role in the trapping and recombination (TR) process in s.-i. material.

The project performance has been conducted in the following main directions:

- EPR investigation of the two sets of 4H s.-i. samples in the dark in the temperature interval from 77 K to 4.2 K. One set is commercial, undoped HPSI 4H-SiC grown by PVT, while the second set is vanadium doped PVT 4H SiC;
- EPR investigation of the undoped HPSI 4H-SiC grown by PVT and vanadium doped PVT 4H SiC after annealing of the samples at 1400 ^{0}C and 1800^{0}C;
- Photo EPR investigation of the of the undoped HPSI 4H-SiC grown by PVT and vanadium doped PVT 4H SiC before and after annealing of the samples at 1400 ^{0}C and 1800^{0}C in the temperature interval from 77 K to 4.2 K;
- The investigation of the EPR spectrum in undoped HPSI 4H SiC samples with application of the photo excitation and photo quenching EPR method in the temperature interval from 77 K to 4.2 K;
- Investigation of the spectral and time characteristics of the photosensitive paramagnetic centers observed in undoped HPSI 4H SiC samples in the temperature interval from 77 K to 140 K;
- Investigation of the temperature characteristics of the photosensitive paramagnetic centers observed in undoped HPSI 4H SiC samples in the temperature interval from 4.2 K to 140 K;
- Multifrequency investigation of the ligand hyperfine structure (HFS) of the defects.

Two EPR spectra of vanadium in the $V^{3+}(3d^2)$ charge state (S = 1, I = 7/2) from the cubic and hexagonal sites in the temperature interval from 4.2 to 77 K has been detected in the dark in the vanadium doped PVT 4H SiC samples. The parameters of the spin Hamiltonian have been obtained from an analysis of the angular dependence of the EPR spectra for a rotation of the magnetic field in the $(11\bar{2}0)$ plane. From the difference in the intensity of the low and high field resonance transitions at 4.2 K and 37 GHz the signs of the fine structure parameters D were determined to be positive for the two V spectra.

Along with EPR spectra of vanadium some samples exhibited EPR spectrum due to Mn^{2+} (I= 5/2, S=5/2) in the dark after etching of the sample in KOH. Only the central hyperfine sextet from Mn^{2+} is observed in EPR spectrum. The fine structure lines are broadened beyond detection probably due to random internal strains in the samples. Manganese has 100% abundant isotope with nuclear spin I = 5/2 and the observed splitting corresponds to that of Mn^{2+} in the $3d^5(^6S_{5/2})$.

Subsequent illumination of the sample with above bandgap UV light EPR spectrum of boron appeared in EPR spectrum of vanadium showing that that vanadium can also be in a paramagnetic state in p-type SiC.

The undoped as-received HPSI 4H SiC samples exhibit EPR signal, labeled I_R in the dark. This single EPR line with S=1/2 was eliminated in samples that were annealed for short time at 1400 ^{0}C. The g-factor and thermal characteristics of the I_R EPR signal are in a good agreement with those for the carbon-related surface defect in 4H SiC with isotropic g-factor ($g_{\|} = g_{\perp} = 2.0025$) which has been studied by Macfarlane and Zvanut [6].

Another EPR spectrum from defect labeled X with S = 1/2 is also observed in all HPSI 4H SiC samples under investigations in the dark. The defect is thermally stable and persists in EPR spectrum after annealing of the sample up to 1800^{0}C. Thus, the position of the Fermi level in the dark in HPSI 4H SiC samples is determined by energy level of the X center. Unfortunately, the ligand hyperfine structure (HFS) was not detectable in spectrum of X center due to the small concentration of the defect, estimated to be about $5\cdot10^{14}$cm^{-3}. This fact hampers the unambiguous identification of the X center.

From the investigation of the temperature behavior of the X center it was found a significant difference in symmetry of the defect residing cubic and hexagonal lattice site. The X center in hexagonal site persists axial symmetry of EPR spectrum in the temperature interval from 77 K to 4.2 K. On the other hand X center in cubic site is characterized by large Jahn-Teller distortion, resulting in breaking of the axial C_{3v} symmetry of EPR spectrum observed at 77 K towards D_{2d} symmetry at low temperature.

The situation was changed when the samples were photo excited. Excitation of the samples with the band gap light results in the transition of the impurities and defects presented in the sample from a diamagnetic ground state into observable paramagnetic state depending from the location of the quasi Fermi level at given temperature.

The series of HPSI 4H SiC s.-i. samples under investigations demonstrates the different position of the quasi Fermi levels in the band gap at given temperature. Excitation of the first type of the samples with UV light at 77 K resulted in the neutralization of the shallow donors and acceptors and as a result the EPR signals from nitrogen and

boron were appeared in EPR spectrum. EPR spectrum of second type of the samples at 77 K consists of EPR signals of boron and nitrogen of small intensity and two additional lines due to the intrinsic defect labeled P residing the two inequivalent lattice sites. The third sample revealed only EPR spectrum of boron and the P defect at 77 K, without the nitrogen spectrum.

As the temperature goes down to the 4.2 K, the quasi-Fermi levels for electrons, , and holes, ϕ_p, fall to the edge of the conduction and valence band respectively. As result, the population of the paramagnetic centers with different energy levels is changed and the transition of the defect centers with shallow energy levels from a diamagnetic ground state into observable paramagnetic state occurs.

Particularly, the intensity ratio of boron EPR lines corresponding to the quasicubic and hexagonal sites at 77 K $I_B^k : I_B^h = 2$ is reversed to 0.5 at 50 K. The EPR line from defect center labeled ND1 appeared in EPR spectrum at 50 K corresponding to the defect with shallow level.

On other hand as the temperature increase from 77 K to 140 K the quasi-Fermi levels for electrons, ϕ_n, and holes, ϕ_p are moving towards the middle of the band gap, as a result, the capture of free carriers becomes more and more efficient on the deep levels which become paramagnetic.

The principle feature of s.-i. material is that the lifetime of the electrons and holes captured on the intrinsic defect and impurity levels is very long of about 10-14 hours and more at low temperature. The metastable state of the photosensitive intrinsic defects and impurities indicate that at low temperature the recombination rate of the photo-created carriers is very small. This phenomena is observed in many semiconductor structures and called persistent photoconductivity [13].

To establishment the recombination mechanism of persistent photo-carriers captured on the deep and shallow levels the time and spectral characteristics of the photosensitive paramagnetic centers have been investigated.

Time characteristics of the photo-carriers captured by nitrogen and boron levels consist of the fast and slow component of decay curves. Due to the similar behavior of the fast component of decay curves of the carrier concentration captured by nitrogen and boron energy levels it could be suggested that the fast component is responsible for the recombination process between nitrogen and boron. Following the Shockley-Read-Hall (SRH) model, the electrons and holes can be successively captured by a single defect level and recombine.

The slow component of decay curves for the photo-carriers captured on the nitrogen and boron levels have the different behavior and could be caused by the existence of trap level in the forbidden band. Electrons from nitrogen energy level recaptured by trap level where the lifetime of the trapped electrons is very long and recombination process between electrons captured by trap and holes captured by boron can be neglected which is supported by slow component for boron center. The charge transfer process occurring between shallow nitrogen and trap level is supported by the time dependence of the decay and rise of the nitrogen and P center EPR resonance lines respectively after band gap excitation light was switched off.

A substantial enhancement of the recombination rate of the photo-created carriers can be achieved by quenching of the sample with the below band gap light of various wavelengths. At the same time independent of the quenching light energy the electrons released from nitrogen energy level is captured by P center where the lifetime of the trapped electrons is very long.

As was shown in Ref. [5] the efficiency of the intercenter charge transfer process in SiC is enhanced by increasing the concentration of deep donors and by lowering the Fermi level to midgap after which the nitrogen donors tends to interact less with the conduction band and more with states below them.

Indeed, the temperature induced cascade intercenter charge transfer process is observed in 4H SiC s.-i. material in the dark preliminary excited by UV light. When the temperature increase and the Fermi level is moving down to the midgap, the free carriers released from shallow donors and acceptors are captured by the level at which the Fermi level is locked at given temperature. As result the electron recapture process by a series closely located energy levels corresponding to the P, L and X intrinsic defects with the difference in energy of $\Delta T = 140\ K - 107\ K = 33\ K = 2.85$ meV has been discovered in 4H SiC s.-i. material.

Convincing identification of the intrinsic defects taking part in recombination and charge transfer process in 4H SiC s.-i. material requires determination of their ionization energy and charge state. The position of the energy level of the defects in the band gap can be estimated from the photon energy of the excitation light at which the intrinsic defects are either excited or quenched in the EPR spectrum.

The investigation of the photo excitation and photo quenching of the EPR spectrum in the HPSI 4H SiC samples shows that photo quenching of X center occurs approximately with the same photon energy threshold as photo excitation of the P center at about $h\nu = 2.1$ eV. It gives possibility to determine the position of the energy levels of the P and X centers at $\Delta E = \Delta E_g - 2.11 = E_C - (1.15 \pm 0.06)$ eV and to make the conclusion that P and X centers are deep donor–like defects. Uncertainty in energy determination of about ≤ 0.06 eV does not allow to distinguish X and P defect levels.

The correlation observed between the decay and rise in intensity of the EPR signals for X and P centers at approximately the same energy could be explained by a charge transfer process between them. The electrons excited by

the light from the X center could be captured on the energy level of the P center via the conduction band.

Taking into account that P center is not observed in the dark, the position of the Fermi level and energy level of X center should be below the energy level of P defect. The situation similar to that which was observed for nitrogen (^{14}N) in 4H and 6H SiC. In spite of a small difference between the energy level of ^{14}N in cubic and hexagonal (h) sites (0.05 eV) appearance and intensity of EPR signal from shallow ^{14}N in h sites strongly depends from the location of the Fermi level [7].

The ND1 defect occurs inside the EPR spectrum of nitrogen in the s.i. sample when illuminated by light with an energy threshold at about hν = 3.19eV (365 nm). Taking the threshold energy as the energetic distance of the ND1 defect from the valence band, one can estimate the position of the energy level of ND1 as $\Delta E = \Delta E_g$ - 3.19 eV = E_C – 0.07 eV indicating that the defect originates from a shallow donor state with an ionization energy between the cubic and hexagonal nitrogen energies.

All defects observed in s.-i. samples in two inequivalent lattice sites with isotropic width and S=1/2 are thermally stable and persist in EPR spectrum after annealing the sample at least up to 1800 ^{0}C, indicating that the intrinsic defects are not a vacancy-related complex since these are not stable up to 1800 ^{0}C.

Unfortunately, the determination of the local symmetry of the nearest neighbor (NN) environment of the intrinsic defects using their ligand hyperfine structure (HF) is not able due to their small intensity. The concentration of the X and P defects estimated from the integrated intensity of their EPR signal is about $5\cdot10^{14}$cm^{-3} and $2\cdot10^{15}$cm^{-3} respectively.

In order to avoid these problems the identification of the intrinsic defects observed in s.i. 4H SiC has been undertaken on as-grown 4H SiC samples in which some of the defects are also present but with higher concentrations.
Two donor paramagnetic states originated from nitrogen and a intrinsic defect have been resolved and studied in n-type 4H SiC bulk material at 9.6 and 140 GHz in the temperature range of 4.2 K to 77 K. Additional small intensity lines symmetrically positioned about the nitrogen and native defect EPR lines were attributed to the four nearest ^{13}C atoms surrounding nitrogen and the native defect using the line intensities and the natural abundance of magnetic isotopes ^{29}Si (4.7%) and ^{13}C (1.1%). A remarkable result is that the value of the ^{13}C isotropic HF interaction constant for nitrogen on the quasi-cubic site was found to be an order of magnitude larger than those determined from ^{29}Si and ^{13}C ENDOR spectra. This fact enabled us to conclude that nitrogen in 4H SiC occupies the silicon site in the lattice and not the carbon site as was previously accepted.

An ionization energy E = 42 meV corresponding to the value of valley - orbit splitting of nitrogen sitting at cubic sites has been obtained. A small energy ionization of E = 4.5 meV obtained for ND1 donor center residing the hexagonal position is also attributed to the value of valley - orbit splitting.

Two paramagnetic intrinsic defects P and ND1 with S=1/2 residing the hexagonal and cubic positions have been resolved and studied in n-type 4H SiC bulk material having deviation from the stoichiometry towards excess of carbon and grown in Sc atmosphere at 140 GHz and 4.2 K.

The observed HF interactions of ND1 with the four NN ^{13}C nuclei proved that ND1 resides on a Si site whereas the presence of a HF interaction with one ^{13}C atom with larger HF splitting than the four NN ^{13}C nuclei indicates that there is a central HF interaction with one ^{13}C. This fact makes it possible to conclude that ND1 involves a C atom occupying a Si site, i.e., a C_{Si} antisite, which has the lowest formation energy in C-rich material [5]. Considering that the defects have spin S = 1/2, C_{3V} symmetry of the EPR spectrum and appear to be donor-like defect is suggested to be the carbon antisite in the single negative charge state (C_{Si}^-). Following the theoretical predictions made in [5] the carbon antisite exists only in the charge-neutral state and there was no experimental evidence up to now to prove its presence in the band gap.

According to the resolved ligand HF interactions with ^{13}C atoms in EPR spectrum of P center and the C-rich growth conditions, the P center has been identified with the silicon vacancy. The Si vacancy is predicted to have a spin S =1/2 ground state for either +1 or -3 charge states[5]. Considering that P defect has spin S = 1/2, C_{3V} symmetry and appear to be donor-like defect P is attributed to the silicon vacancy in the –3 charge state (V_{Si}^{3-}) and photo quenching process for the P defect will be described by the following charge transitions

$$V_{Si}^{3-} - e^- \rightarrow V_{Si}^{2-}.$$

X center which was not detected in as-grown n-type 4H SiC bulk material is tentatively attributed to the V_C^{1-} defects. In accordance with the theoretical predictions made in [8,9] possible identification of the donor-like monovacancies, located in the upper half of the band gap, with the low spin state S =1/2, are the carbon and silicon vacancies in the negative charge states –1 and –3 respectively.

Comparing the EPR parameters for the X center with those for EI5, which has been associated with the carbon vacancy in the positive charge state +1, it could be suggested that the donor-like X center is related to the carbon vacancy in the negative charge state –1. The absence of the EPR signal from V_C^+ in the dark and under photo excitation in HPSI 4H SiC samples under investigation could be explained by the difference in location of the Fermi level and quasi Fermi levels in HPSI 4H SiC samples investigated in [1-3] and in present work.

This conclusion is supported by the fact that X defect in cubic site is subject to a the Jahn-Teller distortion. As follows from theoretical prediction carbon vacancies in neutral or negative charge states are characterized by large Jahn-Teller distortion inward relaxations, resulting in breaking of the T_d symmetry towards D_{2d} symmetry. In addition for the singly negative charge state it was found a significant difference between C vacancies at cubic and hexagonal lattice.

Thus, it was established that in all HPSI 4H SiC samples under investigation Fermi level was pinned at X defect level located in the upper half of the band gap in the dark. All others impurities and defects such as nitrogen, boron and P defect related to the isolated silicon vacancy are in a non-EPR active state. Excitation of the samples with the light gives rise to the transition of them from a diamagnetic ground state into observable paramagnetic state depending from the location of the quasi Fermi level at given temperature. The investigation of the photo excitation and quenching of the EPR spectrum in the HPSI 4H SiC samples shows that the energy level of the P defect is also located in the upper half of the band gap approximately at 1.15 ± 0.06eV below E_C.

The EPR data obtained are confirmed by temperature dependent Hall effect measurements. The Hall effect experiments proves that the sample is n-type and the deep levels pinning the Fermi level are donor-like defects which are present in concentrations of at least $1 \cdot 10^{15}$ cm^{-3}. This can be considered the minimum concentration of the compensating deep donor level and is in the range of the concentrations determined from EPR for the P defect. No evidence for the presence of holes was detected indicating that the Fermi level is pinned in the upper half of the band gap in this material. This suggests that the positively charged carbon vacancy or carbon vacancy complexes located in the lower half of the band gap which were recently detected by EPR in s.i. 4H SiC material [1-3] are probably not responsible for compensation in our material. The V_{Si}^{3-} defect is suggested to be the dominant compensating deep level.

Current status of the project.

The project has been carried out in accordance with the work schedule of the project.

In the reporting period the s.-i. 4H SiC samples grown at the different technology conditions such as growth or annealing temperature, growth velocity, doping level and compensation degree supplied by AFRL/MLPS have been tested with EPR in X-, Q-, D-band in the temperature interval from 4.2 K to 77 K in the dark. Analysis and processing of experimental EPR data have been carried out. The parameters of EPR spectra observed in undoped HPSI 4H-SiC grown by PVT and vanadium doped PVT 4H SiC and n-type 4H SiC samples have been determined. The identification of the EPR spectra has been performed.

Analysis and processing of experimental EPR data have been carried out.

Two EPR spectra of vanadium in the $V^{3+}(3d^2)$ charge state ($S = 1$, $I = 7/2$) from the cubic and hexagonal sites in the temperature interval from 4.2 to 77 K has been detected in the dark in the vanadium doped PVT 4H SiC samples. The parameters of the spin Hamiltonian have been obtained from an analysis of the angular dependence of the EPR spectra. From the difference in the intensity of the low and high field resonance transitions at 4.2 K and 37 GHz the signs of the fine structure parameters D were determined to be positive for the two V spectra.

Along with EPR spectra of vanadium some samples exhibited EPR spectrum due to Mn^{2+} (I= 5/2, S=5/2) in the dark after etching of the sample in KOH. Only the central hyperfine sextet from Mn^{2+} is observed in EPR spectrum. The fine structure lines are broadened beyond detection probably due to random internal strains in the samples. Manganese has 100% abundant isotope with nuclear spin I = 5/2 and the observed splitting corresponds to that of Mn^{2+} in the $3d^5(^6S_{5/2})$. The parameters of Mn^{2+} EPR spectrum in 4H SiC have been determined.

The intrinsic defect ND1 along with nitrogen EPR spectrum has been detected in n-type 4H SiC AN0109-03 sample. Analysis of ligand hyperfine structure observed in EPR spectrum of nitrogen has been performed in X-band (~9.6 GHz), Q- band (~37 GHz) and D- band (~140 GHz) which enable us to conclude that nitrogen substitutes the silicon site in the lattice and not the carbon site as was previously accepted. The value of valley - orbit splitting for ND1 donor center residing the hexagonal position and nitrogen sitting at cubic site have been determined from the analysis of their temperature characteristics.

The samples have been measured before and after annealing in an inert atmosphere in the temperature range of 1400 ^{0}C - 1800 ^{0}C. For this purpose installation for thermal rapid annealing of 5 x 5 mm size sample with heating rate 800-1000^{o}C in sec and minimum duration of one stage (step) of an annealing 10 sec has been elaborated. Thermal annealing has been performed in the He flow. These conditions completely ruled out possibility for epitaxial film formation on the crystal surfaces. The annealing temperature T_{ann} varied from 1400 up to 1800 °C; it was monitored with an optical pyrometer.

The photo-EPR method including photo excitation and photo quenching technique has been developed for the investigation of the spectral and time characteristics of the photosensitive paramagnetic centers in s.-i. SiC.

The parameters of the photosensitive paramagnetic centers observed in s.-i. 4H SiC samples have been determined. The identification of the EPR spectra observed in s.-i. samples has been performed. It was established that the behavior of the s.-i. SiC samples under excitation with the UV light strongly depends from the history of the sample: Fermi level, concentration of donors. A shallow nitrogen donor, shallow boron acceptor and four intrinsic defects including ND1, P, X and L centers have been discovered in undoped HPSI 4H-SiC samples in two inequivalent lattice sites under illumination of the samples with the light.

The spin, charge state, energy levels and symmetry of the EPR spectrum of defects have been determined. From the spectral dependencies of the defects the position of the energy level of P, X and ND1 defects in the band gap have been determined. It was established that all intrinsic defects in undoped HPSI 4H-SiC samples under investigations are located in the upper half of the band gap.

The concentration of the X and P defects of about $5 \cdot 10^{14}$$cm^{-3}$ and $2 \cdot 10^{15}$$cm^{-3}$ respectively has been estimated from the integrated intensity of their EPR signal.

The identification of the intrinsic defects P and ND1 has been proposed on the base of spin, charge state, energy levels, symmetry of the EPR spectrum, resolved ligand hyperfine interactions with nearest environment, preparation conditions of the samples, temperature stability of the defects and theoretical prediction. P center has been attributed to the isolated vacancy on silicon sites in the charge states -3. ND1 center is attributed to the carbon antisite in the single negative charge state.

Investigations of the temperature characteristics of the photosensitive paramagnetic intrinsic defects have been performed. It enables to discover the temperature induced cascade intercenter charge transfer process in undoped HPSI 4H-SiC material in the dark preliminary excited by UV light. The recapture process of free electrons by a series closely located energy levels corresponding to the P, L and X intrinsic defects with the difference in energy of ΔT = 140 K – 107 K = 33 K = 2.85 meV has been observed in 4H SiC s.-i. material.

The spectral and time characteristics of the photosensitive paramagnetic centers have been investigated. The recombination mechanism of persistent photo-carriers captured on the deep and shallow levels has been proposed. The charge transfer process occurring between shallow nitrogen and trap level corresponding to the P center has been discovered. It was established that time characteristic of the photo-carriers captured by nitrogen and boron levels consist of the fast and slow component of decay curves. Two components of decay curves for the photo-carriers captured on the nitrogen and boron levels have been described by kinetic equations.

The EPR data obtained are confirmed by temperature dependent Hall effect measurements. The conclusion about the nature of the dominant compensating deep level in undoped HPSI 4H-SiC material has been made on the basis of the comparison EPR and Hall data obtained. It was concluded that deep levels pinning the Fermi level in undoped HPSI 4H-SiC material are donor-like defects namely P and X defects which are present in concentrations of at least $1 \cdot 10^{15}$ cm^{-3}.

Summary of personnel commitment.

Participants SPI	*Activities*
Kalabukhova K.	1.1, 1.4, 2.1, 2.2, 2.4, 3.1, 3.2, 3.3, 4.1, 4.2, 4.3, 4.4
Lukin S.	1.1, 1.2, 2.1, 2.2, 2.4, 3.1, 3.2, 3.3, 4.1, 4.2, 4.3, 4.4
Savchenko D.	1.4, 1.5, 2.4, 2.5, 3.3, 3.4, 4.3, 4.4, 4.5
Venger E.	2.4, 3.3, 4.4
Kiselev V.	1.3, 2.3
Avramenko S.	1.3, 2.3
Amirhanov D.	1.1, 1.2, 1.4, 2.1, 2.2
Kolesnik S.	1.1, 2.1, 2.2
Sitnikov O.	1.1, 2.1, 3.1, 3.2, 4.1, 4.2, 4.3

Kalabukhova K. was mostly involved in X-, Q-, D- band EPR measurements of 4H SiC s.-i. materials, analysis and processing of experimental EPR data, preparation of the quarter reports, papers, talks and the materials for the conferences.

Lukin S. was mostly involved in X-, Q-, D- band EPR measurements of 4H SiC s.-i. materials, assembly, adjustment of the photo- EPR technique including the photo-excitation and photo-quenching EPR method, investigation of the spectral, time and temperature characteristics of the photosensitive paramagnetic centers in s.-i. SiC, analysis and processing of experimental EPR data.

Savchenko D. was mostly involved in analysis and processing of experimental EPR data, developing of working documentation, preparation of the quarter reports, papers, talks and the materials for the conferences.

Venger E. was mostly involved in analysis and processing of experimental EPR data. Comparison of the data obtained by EPR with that obtained by electrical and optical methods in AFRL/MLPS laboratory.

Kiselev V. and Avramenko S. were mostly involved in preparation of the technology base for the sample annealing, preparation of the working sample and annealing of the s.-i. SiC samples in the temperature range from 1400 to 1800 C.

Amirhanov D. and Sitnikov O. were mostly involved in assembly, adjustment of the photo- EPR technique including the photo-excitation and photo-quenching EPR method, tuning and operation of the X-, Q-, D- band EPR spectrometers.

Description of travels.

1. Participants: Kalabukhova E.N

Purpose: Participation in the International European Conference on Silicon Carbide and Related Materials, Linkoping, Sweden, September 1-5, 2002

Main result: Publication. Kalabukhova E.N., Lukin S.N., Mitchel W.C Electrical and Multifrequency EPR Study of Nitrogen and Carbon Antisite Related Native Defect in n-Type as-Grown 4H-SiC European Conference on Silicon Carbide and Related Materials (ECSCRM - 2002, Sweden, Linköping) Mat. Sci. Forum 2003. - 433-436. - P. 499-502.

2. Participants: Kalabukhova E.N

Purpose: Participation in the International European Conference on Defects in Semiconductors Aarhus Denmark, July 27-August 2, 2003

Main result: Publication. Kalabukhova E.N., Lukin S.N., Savchenko D.V., Mitchel W.C. "Electrical and multifrequency EPR study of nonstoichiometric defects in 4H-SiC" The 22 nd International Conf. on Defects in Semiconductors (ICDS -2003, Aarhus, Denmark) Physica B, 2003. - 340-342C. - P. 156-159.

Information about major equipment and materials acquired, other direct costs, related to the project.

Equipment

Description	Cost $
Auxiliary equipment	420
Printer	100
Computer	1350
Monochromator	400
Laboratory furniture	100

Materials

DESCRIPTION	Cost $
Stationary	500
Radiocomponents	240
Cartridge	120

Other Direst Costs

DESCRIPTION	Cost, $
Communication (Internet)	470
Computer service	160

Table Redirection

Reference documents &date (1)	*New requested category,* or old category with new cost (2)	Requested cost (new) (3)	*Original (old) category (4)*	*Estimated cost (old)* (5)	Redirected cost (6) *old – new*
		Quarter <02>			
L02 26.06.02	*Travel to Linkoping, Sweden for Participation in the International European Conference on Silicon Carbide and Related Materials*	*2157*	*Travel to Germany, Paderborn*	*2000*	*+157*
			Liquid helium	*157*	*-157*
		Total by L02			*0*
		Quarter <03>			
L02 17.02.03	*Fax KX-FL503*	*377*	*Fax*	*300*	*+77*
			Computer service	*163*	*-77*
		Total by L02			*0*
		Quarter <04>			
19.03.03	*Engineer Kolesnik Sergei (daily rate 20 $ of time 34%)*	*2060*	*Engineer Sitnikov Olexandr(daily rate 20 $ of time 34%)*	*2060*	*-2060*
		Total			*0*
		Quarter <05>			
L03 23.06.03	*Travel to Aarhis Denmark for Participation in International European Conference on Defects in Semiconductors*	*2283*	*Liquid helium*	*780*	*-2283*
			Liquid nitrogen	*800*	
			Computer software	*400*	
			Computer service	*63*	
			Communication	*240*	
		Total by L03			*0*
		Quarter <06>			
L04 30.09.03	*Monitor TFT 17'*	*434*	*Computer PC Athlon 1.5 GHz*	*1260*	*-1260*

	Computer Advantis XN5f2.4/256DDR/40G/CD52/64	*109*			
	Monitor 15' Samsung	*109*			
Total by L04					*0*
Quarter <06>					
L06 30.09.03	*Software MICROSOFT MS Windows XP Home Rus w/SP1a*	*81*	*Computer software*	*81*	*-81*
Total by L06					*0*
Quarter <06>					
L05 06.10.03	*Scanner Org/Scan MUSTEK*	*83*	*Computer service*	*83*	*-83*
Total by L05					*0*
Quarter <08>					
L05 16.06.04	*ComputerP4/2.8Ghz/865G/512Mb/ 120Gb/1.44Mb/Video /SB/NET/CD-RW/Keyboard Genius/Mouse MITSUMI/WIN XP RUS/Office SB XP RUS*	*1009*		*0*	*+1009*
	Printer HP LaserJet 1300	*326*		*0*	*+326*
	Fax-modem GVC 56K SF 1156V/R21 Plus	*58*		*0*	*+58*
	Monitor 17'' Samsung 173 T TFT	*552*		*0*	*+552*
	USB Flash Drive256Mb	*75*		*0*	*+75*
L03 23.06.03 *L02 26.06.02*			*Liquid helium*	*1440*	*-1440*
L05 16.06.04	*Liquid helium*	*0*			
L03 23.06.03			*Liquid nitrogen*	*1000*	*-580*
L05 16.06.04	*Liquid nitrogen*	*580*			
					2020
Total by L05					*0*

! *Note. After the hard copy of this document, attach copies of technical reports (milestones), completed to the date. Associated files should be collected in the directory "**Annual_0/Final**". >*

Title of the Project: **"Photo EPR study of trapping and recombination processes in semi-insulating 4H, 6H SiC crystals over a wide temperature interval".**

Project manager: Kalabukhova Kateryna Mykolaevna, Doctor
Phone: 38 044 265 62 97
Fax: 38 044 243 48 93
E-mail: katia@i.kiev.ua
Institutions: Institute of Semiconductor Physics National Academy of Science of Ukraine (NASU)
Financing parties: USA, European Office of Aerospace Research & Development EOARD
Operative commencement date: March 1, 2002
Project duration: March, 2002 –May, 2004
Project technical area: Basic Science
Reported : 01.03.2002 – 31.05.2004
*Date of submission:*14.07.04

Executive summary

The main obstacle to SiC becoming a widespread semiconductor material is the problem arising from high-quality large-area crystal growth with controlled incorporation of dopants and intrinsic defects. Therefore to tailor the properties of a semiconductor in a desired way, the electronic structure and the stability of the intrinsic defects must be well understood. A thorough understanding of the recombination processes in semiconductors is also of great importance, the recombination rate via different channels determines the minority carrier lifetime, which is a key parameter that limits the performance of many semiconductor devices. The results obtained in the present project is directly applied to solve that problem.

The project is devoted to the multifrequency Electron Paramagnetic Resonance (EPR) and photo EPR study of the intrinsic defects and impurities responsible for the semi-insulating (s.-i.) properties SiC material and mechanism of trapping recombination process occurring in s.-i. SiC material to be able to adjust and optimize the growth parameters of s.-i. SiC large wafers. The investigation of paramagnetic intrinsic defects in s.-i. 4H, SiC has been carried out through measurements of the EPR spectrum at three microwave frequencies 9, 37, 140 GHz in the dark and under photo excitation, before and after annealing of the samples in the temperature interval from 1400 C to 1800 C. To determine the energy characteristics of intrinsic defects, the EPR spectra have been studied in the wide temperature interval from 77 K to 4.2 K in the dark and under illumination of the sample with the light in the range of 360-900nm.

The influence of the different growth parameters such as stochiometry, doping level and degree of compensation on the behavior of EPR spectra have been studied. The correlation between the concentration, type of the intrinsic defects and technology condition of of s.-i. SiC preparation has been established that can be used for developing of the s.-i. SiC technology growth with controlled incorporation of dopants and intrinsic defects. The fact that the intrinsic defect originating from deviation of the stoichiometry towards the carbon excess has been detected in undoped high purity semi-insulating (HPSI) 4H SiC samples shows that commercial available undoped high purity s.i. materials are grown with deviation of stoichiometry.

The different position of the quasi Fermi levels that have been revealed in a series of HPSI 4H SiC samples at given temperature shows that the samples have different degree of compensation and different concentration of the deep intrinsic defects. The temperature behavior of the quasi Fermi levels in HPSI 4H SiC samples has been also studied.

Microscopic models for dominant deep intrinsic defects responsible for the semi-insulating properties of the SiC material has been proposed on the base of EPR spectrum symmetry, the hyperfine structure due to the interaction with adjacent Si (C) neighbors, and the energy, charge, spin characteristics of the defects. The theoretical value of the formation energies, ionization levels, geometries and charge states of the relaxed structures for the defects residing hexagonal and cubic lattice site have been take into consideration to confirm the identification of the intrinsic defects.

The data about the electronic structure and energy characteristics of the dominant deep levels responsible for the semi-insulating properties of the SiC material can be applied for developing of general principles of growing s.-i. single crystals of ever increasing diameter and quality that will promote a low cost yield of s.-i. SiC wafers.

The investigation of carrier recombination process in s.-i. SiC and identification of the intrinsic defects, impurities involving into the donor acceptor recombination process has been performed through the photo-EPR methods including photo-excitation and photo-quenching technique and investigation of the spectral and time characteristics of the photosensitive paramagnetic centers. The long living state of the free carriers captured by impurities and intrinsic defects has been discovered in s.-i. SiC material. This phenomena is observed in many semiconductor structures and called persistent photoconductivity. The charge transfer process occurring between

shallow nitrogen and deep trap levels has been detected. In addition the temperature induced cascade charge transfer process between deep levels of intrinsic defects has been observed in 4H SiC s.-i. material in the dark preliminary excited by UV light The nature of the life time controlling intrinsic defect in s.-i. SiC material has been identified.

The electronic model of the free carrier recombination process in s.-i. SiC material has been proposed.

The project has been undertaken in close collaboration with the Air Force Research Laboratory, Materials and Manufacturing Directorate, AFRL/MLPS, Wright-Patterson Air Force Base, Ohio which is engaged in electrically and optically characterization of SiC material. The correlation between electrical, optical and EPR data has been established.

The advantage of the project is that the high resolution magnetic resonance methods have been applied to the investigations of intrinsic defects in SiC, which greatly enhances the sensitivity and spectral resolution of magnetic resonance techniques. Moreover the hyperfine ligand structure for intrinsic defects could be better recognized and identified using the multifrequency EPR measurements.

Cooperation with foreign collaborators

The project has been undertaken in collaboration with the Air Force Research Laboratory, Materials and Manufacturing Directorate, AFRL/MLPS, Wright-Patterson Air Force Base, Ohio which is engaged in electrically and optically characterization of SiC material. The correlation between electrical, optical and EPR data has been established.

Publications

1. Kalabukhova E.N., Lukin S.N., Saxler A, Mitchel W.C., Smith S R., Solomon J.S. Evwaraye A. O. //Photo EPR Study of Trapping and Recombination Processes in Semi-Insulating 4H-SiC Crystals as Function of Temperature // MRS Symp. Proc. Vol. 680E, P. E9.4.1 - E 9.4.6, 2001

2. Kalabukhova E.N., Lukin S.N., Mitchel W.C. //Electrical and Multifrequency EPR Study of Nitrogen and Carbon Antisite Related Native Defect in n-Type as-Grown 4H-SiC // Mat. Sci. Forum Vols. 433-436, 499-502, 2003.

3. Kalabukhova E.N., Lukin S.N., Saxler A, Mitchel W.C., Smith S. R., Solomon J.S. Evwaraye A.O.//. Photosensitive EPR spectra in semi-insulating 4H - SiC crystals // Phys. Rev. B. 64, 235202-(1-5), 2001.

4. Kalabukhova E.N., Lukin S.N., Mitchel W.C., Saxler A, R.L. Jones //EPR and photoluminescence studies of semi-insulating 4H-SiC samples// Physica **B 308-310,** p.698-701, 2001.

5. Kalabukhova E.N., Lukin S.N., Savchenko D.V., Mitchel W.C. "Electrical and multifrequency EPR study of nonstoichiometric defects in 4H-SiC" Physica B **340-342C**, p. 156-159, 2003.

6. Kalabukhova E.N., Lukin S.N., Savchenko D.V., Mitchel W.C., Mitchel W.D. Photo EPR and Hall measurements on undoped high purity semi-insulating 4H-SiC substrates// International Conference on Silicon Carbide and Related Materials, ICSCRM - 2003, eds. Roland Madar, Jean Camassel and Elisabeth Blanquet (Trans Tech Publications, Switzerland, 2004) or Materials Science Forum Vols. 457-460, pg. 501 (2004).

Prospects of future development.

The future development of the project results is planning to be on the base of the extension cooperation work with the project Collaborator and SiC Technology companies in the framework of the international projects. CRDF project "High Frequency/High Field (HF/HF) EPR and electrical study of the defect formation mechanism in 4H and 6H SiC wafers with deviation in stoichiometry" has been applied in cooperation with Air Force Research Laboratory, Materials and Manufacturing Directorate, AFRL/MLPS, Wright-Patterson Air Force Base, Ohio and Bandgap Technologies Inc., Columbia, South Carolina, USA, which is currently developing bulk monocrystalline SiC wafers of ever increasing diameter and quality. The project deals with EPR detection and identification of intrinsic defects and deformations caused by deviation of Si/C ratio from stoichiometry in Si-, C - rich 4H, 6H SiC to be able to adjust and optimize the growth parameters of SiC ingots.

At the same time taking into account that a number of Material Science and radiospectroscopy laboratories are intended to the collaborative work with High Frequency Electron Paramagnetic Resonance Research laboratory of Institute of Semiconductor Physics National Academy of Science of the Ukraine, the project "Establishment of the International Scientific and Training High Frequency Electron Paramagnetic Resonance Research Center in Ukraine" has been applied to STCU.

Foreign Collaborators:

1. Air Force Research Laboratory Wright-Patterson Air Force Base Ohio 45433; Sensor Materials Branch Survivability and Sensor Materials Division
Dr. William Mitchel

2. Department of Chemistry North Carolina State University, USA, 27695-8204, North Carolina, Campus Box 8204; Raleigh, NC 27695-8204
Dr. Alex I. Smirnov, Assistant Professor

Project manager

Kalabukhova K. M.

For the Coordinating Institution

V. Lashkaryov Institute of Semiconductor Physics National Academy of Science of Ukraine

Approved
V.F. Machulin

Director of V. Lashkaryov Institute of Semiconductor Physics National Academy of Science of Ukraine

1.1. X-, Q-, D-band EPR measurements of n-, p-type 6H SiC, 4H SiC s.-i. crystals grown at the different technology conditions such as growth or annealing temperature, growth velocity, doping level and compensation degree (T_g, V_g). The samples are supplied by AFRL/MLPS

20 pieces of 4H SiC s.-i. samples grown at the different technology conditions and supplied by AFRL/MLPS have been tested with electron paramagnetic resonance spectroscopy (EPR). The results of EPR testing of the samples are collected in the Table 1.1.1 – 1.1.3.

The EPR measurements have been performed in the dark in the temperature interval from 77 K to 4.2 K in X-, Q-, D-band. The measurements were performed before and after annealing of the samples in the temperature range of 1400 ^{0}C - 1800 ^{0}C.

Fig. 1.1.1 shows a typical EPR spectrum for undoped high purity semi-insulating (HPSI) 4H-SiC samples measured in the dark at ν = 37 GHz, T = 77 K before (a) and after (c) annealing of the sample at T = 1400^{0}C for two orientation of the magnetic field with respect to the **c**-axis: **B** ⊥ **c**, **B** ‖ **c**. As was shown from Fig. 1.1.1, the unannealed HPSI 4H-SiC samples revealed two EPR lines in the dark at 77 K. One broad EPR line labeled I_R with isotropic g-factor $g_\| = g_\perp = 2.0025$ which is completely vanished in EPR spectrum after a short (4min) anneal in an inert atmosphere at 1400 ^{0}C and second EPR line, labeled X, which is thermally stable and persists in EPR spectrum after annealing of the sample up to 1800^{0}C. The X line is split into two lines when the magnetic field **B** is parallel to the **c**-axis. At 77 K two EPR lines, X_h and X_c, have axially symmetric g-factors, isotropic width and correspond to the two inequivalent sites of the defect center with S=1/2. Thus, the position of the Fermi level in the dark in undoped HPSI 4H SiC samples is determined by energy level of the X center. When the temperature decrease up to 40 K the transformation of one single line X_c into six EPR lines is occured showing that the symmetry of EPR spectrum is changed from axial C_{3v} to monoclinic symmetry for the defect residing cubic site, see Fig.1.1.2. The behavior of the X defect EPR spectrum is typically for the center with Jahn-Teller distortion.

Vanadium doped PVT 4H SiC samples besides I_R line revealed the EPR spectra of vanadium in the $V^{3+}(3d^2)$ charge state (S = 1, I = 7/2) from the cubic and hexagonal sites in the temperature interval from 4.2 to 77 K in the dark. Fig. 1.1.3 shows the angular dependence of vanadium $V^{3+}(3d^2)$ EPR spectra (S = 1, I = 7/2) from the cubic and hexagonal sites for a rotation of the magnetic field in the $(11\bar{2}0)$ plane measured on s.-i. 4H SiC sample J57-5 at T =77 K, ν = 37 GHz.

BH0429-12 s.-i. 4H SiC sample, annealed at 1800^0 C, revealed two EPR lines from X- center with $g_\|^1$ = 2.0025, $g_\perp^1$ = 2.0044 for X_1- line and with $g_\|^2$ = 2.0028, $g_\perp^2$ = 2.0043 for X_2 - line in the dark. In addition EPR spectra of vanadium in the $V^{3+}(3d^2)$ charge state (S = 1, I = 7/2) from the cubic, hexagonal sites and EPR spectrum due to Mn^{2+} (I= 5/2, S=5/2) has been detected at 77 K and 37 GHz. Fig. 1.1.4. shows EPR spectrum of Mn^{2+} and $V^{3+}(3d^2)$ detected in BH0429-12 crystals of large size. Only the central hyperfine sextet from Mn^{2+} is observed in EPR spectrum, see Fig. 1.1.5. The fine structure lines are broadened beyond detection probably due to random internal strains in the samples. Manganese has 100% abundant isotope with nuclear spin I = 5/2 and the observed splitting corresponds to that of Mn^{2+} in the $3d^5(^6S_{5/2})$.

EPR investigations of n-type and mid n-type 4H SiC samples have been performed at the X-band (~9.6 GHz), Q- band (~37 GHz) and D- band (~7140 GHz) frequencies in the temperature interval of 4.2 - 77 K.

Fig.1.1.6 shows EPR spectrum observed in mid n-type 4H SiC sample (N0109-3) measured at three frequencies at 4.2 K. EPR spectrum consists of a hyperfine structure line triplet corresponding to the nitrogen in quasi-cubic position (N_c) and single ND1-line, which is easily recognized at higher frequency. Whereas the intensity of the ND1-line is the same order of magnitude as that of nitrogen in quasi cubic site, a weak EPR signal of nitrogen in hexagonal site (N_h) could be only resolved at 140 GHz. The single ND1 EPR line has axially symmetric g-factor $g_\|$ = 2.0063(1), $g_\perp$=2.0006(1), isotropic width and corresponds to the defect center with S = 1/2.

Both nitrogen and ND1 - lines accompanied by two satellites as indicated by arrows in Fig. 1.1.6. The satellites are not vanish with increasing the frequency and the distances between them retain when measuring at X-, Q-, D-band frequencies, confirming that they are due to the hyperfine structure (HFS), but not forbidden transitions or the fine structures of a center with spin S = 1.

In two n-type 4H SiC samples (AN 0013-9 D1, AM0168-05 D6) EPR spectrum of nitrogen in cubic site $\boldsymbol{I_c^N}$ and single EPR line from native defect ND1 were observed in the temperature interval from 4.2-60 K. With increasing the temperature the EPR spectrum is transformed into one broad single line $\boldsymbol{I_S^N}$ with anisotropic g-factor at

77 K: $g_{||}$ = 2.0067, $g_{\perp}$= 2.0012 while the EPR line from native defect ND1 decreased in intensity and disappeared at 62 K.

The 6H SiC E 1062-10 revealed in the dark EPR spectrum of boron on cubic and hexagonal position with the concentration of about $5x10^{17}cm^{-3}$.

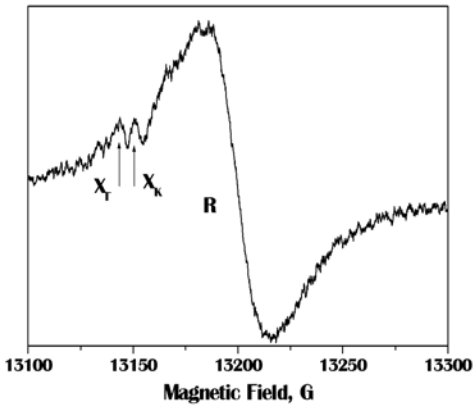

Fig.1.1.1. EPR spectrum observed in the dark for BH0429-09 (D17), AV0609-06 (D21), CL0305-07 (D22) and DC0184 –17(D23) samples. T = 4.2 K, **B** || **c**.

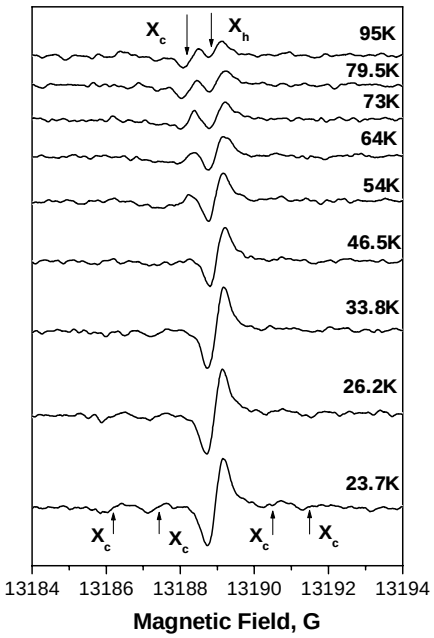

Fig. 1.1.2. Temperature transformation of X defect EPR spectrum. **B** || **c**.

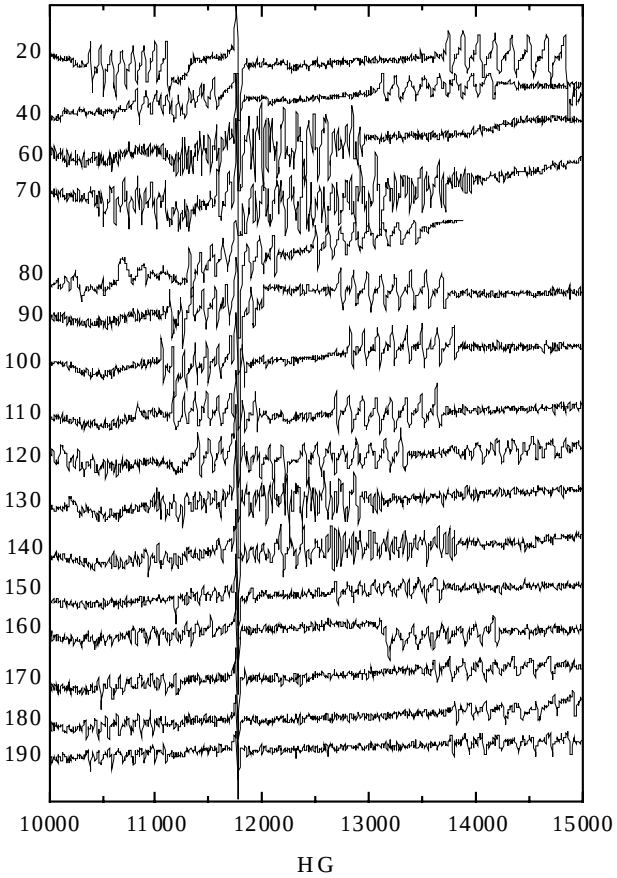

Fig. 1.1.3. Angular dependence of vanadium $V^{3+}(3d^2)$ EPR spectra (S = 1, I = 7/2) from the cubic and hexagonal sites for a rotation of the magnetic field in the $(11\bar{2}0)$ plane measured on s.-i. 4H SiC sample J57-5. T =77 K, ν = 37 GHz.

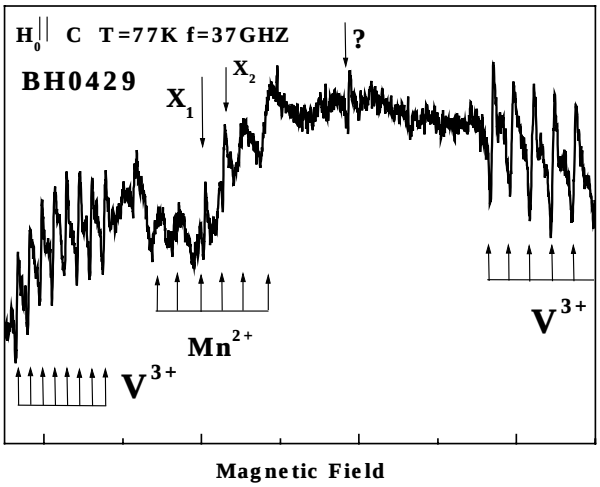

Fig. 1.1.4. EPR spectrum of Mn^{2+} and $V^{3+}(3d^2)$ detected in BH0429-12 crystals of large size.

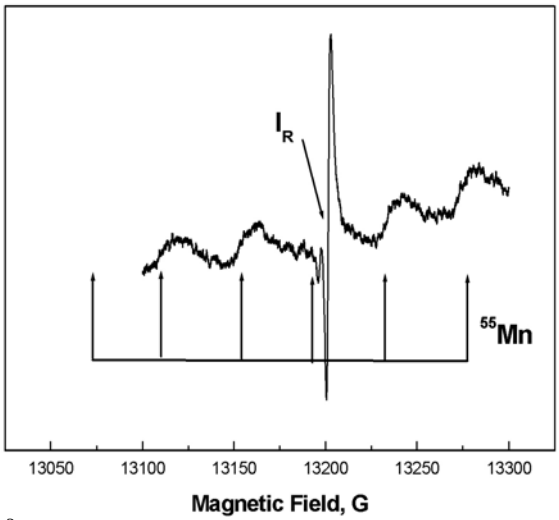

Fig. 1.1.5. EPR spectrum of Mn^{2+} (I= 5/2, S=5/2) observed in s.-i. 4H SiC (CJ112-06 D12) sample in the dark after etching of the sample in KOH. T = 77 K.

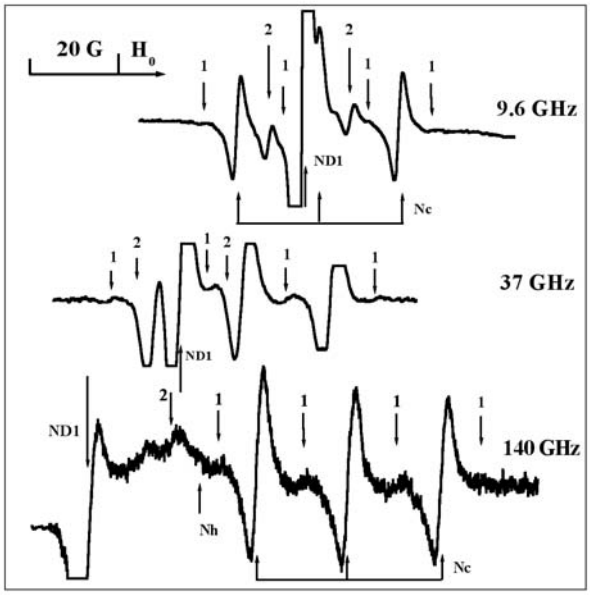

Fig. 1.1.6. EPR spectrum of n-type 4H SiC (sample N0109-3), measured at three frequencies. $\mathbf{B}_0 \| \mathbf{c}$, T = 4.2 K
1- ^{13}C satellite lines related to nitrogen (N_c), 2 - ^{13}C satellite lines related to ND1 defect

Table 1.1.1. Characteristics of the 4H, 6HSiC samples tested with EPR.

Sample	Type	Energy level	Concentration	ν, GHz	T, K	Dark EPR spectra
J57-5 D10 $T_{annel.}$=1600^{0}C	s.- i.		V: 8x10^{16} Ti: 6x10^{17}	37	60-4.2	V^{3+} (S = 1, I = 7/2)
F0648-8 D3	s.- i.	1.6 eV		37	77-4.2	I_R
F0648-8 $T_{annel.}$=1600^{0}C D3	s.- i.	1.6 eV		37	70	-
F0847-4 D4	s.- i.	1.1eV		37	77	I_R, I_X
F0847-4 $T_{annel.}$=1400^{0}C D4,	s.- i.	1.1eV		37	77-50	I_X
Q0407-1 Cree D9	s.- i.		V:1.3x10^{16} Ti:6x10^{16} R =1.7x10^{3}Ωcm	37	77	I_c^B, I_h^B
AW0443-03 D13	s.- i	1.5eV	(vanadium)			
E 1062-10 D20	6H SiC		Ti:6x10^{15} V:1.3x10^{15}	9.6; 37	4.2-77	I_c^B, I_h^B
J70-71 D5	s.- i.	1.6 eV		37	77	I_X
AV0609-06 (D21),	s.- i.	1.1eV		37	4.2	I_R, I_X
CL0305-07 (D22)	s.- i.	low micropipes		37	4.2	I_R, I_X

10/14/04

In charge *Date* *Signature*

POf *S. Sljusarenko, Ph.D*

Table 1.1.1. Characteristics of the 4H, 6HSiC samples tested with EPR.

N	type	Energy level	Concentration	ν, GHz	T, K	Dark EPR spectra
F0575-5 D7	s.-i., Ti/Al contact	1.6 eV	Ti- free, Ti – low, V – high	37	4.2-77	I_R, $\boldsymbol{I_X}$
Q0405-08 D11 $T_{an.}$=1800	s.- i.	1.1eV	V:3.2x 10^{16}	37	77-4.2	$\boldsymbol{I_X}$,
AR0251-16 D8 $T_{an.}$=1600	s.- i.			37	65-4.2	$\boldsymbol{I_X}$? or $\boldsymbol{I_c^B}$?
CJ112-06 D12	s.- i.		V undetected	37	77	$\boldsymbol{I_X}$ $\boldsymbol{I_R}$ Mn^{2+} $3d^5(^6S_{5/2})$
CJ112-06 D12 $T_{an.}$=1800	s.- i.		V undetected	37	77-4.2	$\boldsymbol{I_X}$ Mn^{2+} $3d^5(^6S_{5/2})$
BH0429-12 D17,18,19	s.- i.	1.1eV	V:5.7x 10^{15} Cr:1.9x10^{17}	37	77	$\boldsymbol{I_X}$ $\boldsymbol{I_R}$, $\boldsymbol{V}^{3+}$ (S = 1, I = 7/2) Mn^{2+} $3d^5(^6S_{5/2})$
BH0429-12 D17-19 $T_{an.}$=1800	s.- i.	1.1eV	V:5.7x 10^{15} Cr:1.9x10^{17}	37	4.2-77	$\boldsymbol{I_X}$ $\boldsymbol{V}^{3+}$ (S = 1, I = 7/2) Mn^{2+} $3d^5(^6S_{5/2})$
K126-6 D2	s.- i.	1.1eV	Ti:6x10^{17}	37	77	$\boldsymbol{I_R}$ Trace amounts of $V^{3+}(3d^2)$ Mn^{2+} $3d^5(^6S_{5/2})$
K126-6 D2	s.- i.	1.1eV	Ti:6x10^{17}	140	4.2	Trace amounts of $V^{3+}(3d^2)$ Mn^{2+} $3d^5(^6S_{5/2})$
DC0184-17 D23	s.- i.			37	77	I_R, $\boldsymbol{I_X}$

Table 1.1.1. Characteristics of the 4H, 6HSiC samples tested with EPR.

N	type	Energy level	Concentration	ν, GHz	T, K	Dark EPR spectra
AM0168-05 D6	n-type	E_{d1} = 47meV E_{d2}=85meV E_{d3}=400meV	N_a:4.11x10^{16} N_{d1}:1.04x10^{17} N_{d2}:0.83x10^{17} N_{d3}:5 x 10^{16}	37	77-64	I_S^N , I_c^N
AM0168-05 D6	n-type	E_{d1} = 47meV E_{d2} = 85meV E_{d3}=400meV	N_a=4.11x10^{16} N_{d1}=1.04x10^{17} N_{d2}=0.83x10^{17} N_{d3}=5x10^{16}	37	56 – 4.2	I_c^N , ND1
AN 0013-9 D1	n-type	E_{d1}=44meV E_{d2}=83meV E_{d3}=309meV	N_a=5x10^{16} N_{d1}=1.93x10^{17} N_{d2}=1.8x10^{17} N_{d3}=2.01x10^{17}	37	77	I_S^N (30.09.02) $g_{\|}$=2.0067 $g_{\perp}$=2.0012
AN 0013-9 D1 $T_{annel.}$=1400	n-type	E_{d1}=44meV E_{d2}=83meV E_{d3}=309meV	N_a=5x10^{16} N_{d1}=1.93x10^{17} N_{d2}=1.8x10^{17} N_{d3}=2.01x10^{17}	37	4.2	I_c^N , ND1
N0109-3 D15	mid n-type	40meV 80meV	Ti: 1x 10^{16} Cr: 2.3x10^{16} V: 2.5x10^{14}	9.6; 37; 140	4.2	I_c^N , ND1 ^{13}C
AN0109-03 D16	mid n-type	40meV 80meV	Ti:1x 10^{16} Cr:2.3x10^{16} V:2.5x10^{14}	9.6; 37; 140	4.2	N_c, ND1, ^{13}C
AM0251-03 D14 contacts	low n-type undoped V undetected	E_{d1}=48meV E_{d2}=97meV E_{d3}=576meV	N_a=4.6x10^{16}; N_{d1}=5.1x10^{16} N_{d2}=4.29x10^{16} N_{d3}=1.46x10^{16}			

1.2. Assembly, adjustment of the photo-EPR technique including the photo-excitation and photo-quenching EPR method.

Block-diagram of *Q*-band EPR spectrometer equipped with additional optical arrangement for illumination of the sample in the cavity is shown in Fig. 1.2.1.

Two light sources have been used for the sample illumination in the cavity. For the excitation measurements a mercury high-pressure vapour lamp (250 W) with combination of the interference filter of 380 nm wavelength corresponding to the band-gap width in 4H SiC (3.26 eV) has been used. With a collecting lenses the light was focused on the sample fixed on the end of quartz rod which was simultaneously used as a light guide and placed in resonator. The crystal oriented in such way that the growing axis **c** was perpendicular to the magnetic field.

The quenching light was provided by a 100 W xenon lamp combined with interference filters or glass filters in the wavelength range of 380 nm to 1000 nm. The quenching experiments have been performed with a 100 W xenon lamp combined with prismatic monochromator for a wavelength range of 380 nm to 1000 nm. With this arrangement it was possible to obtain continuous quenching spectra.

A special facility has been elaborated for the illumination the sample in the cavity for **B** || **c** orientation of magnetic field.

1.3. Preparation of the technology base for the annealing the samples in the temperature interval between 1400 C and 1800 C.

The installation for thermal rapid annealing of 5 x 5 mm size sample with heating rate 800-1000^{o}C in sec and minimum duration of one stage (step) of an annealing 10 sec has been prepared.

Rapid annealing has been made with a strip heater. It enabled us to perform thermal annealing with heating rate of up to 1500 $^{\circ}$C/s and minimal annealing stage duration of 5 s. Thermal annealing has been performed in the He flow. The annealing temperature T_{ann} varied from 1400 up to 1800 $^{\circ}$C; it was monitored with an optical pyrometer.

Long-term annealing was made in the Ar atmosphere at a pressure of (0.9–1.0) $\times 10^5$ Pa in a vacuum oven Redmet - 30. The maximal heating rate was 50−100 $^{\circ}$C/min. The crystals were put into a graphite crucible previously saturated with silicon and silicon carbide. This eliminated the possibility of SiC dissociation. On occasion, however, we observed formation of thin epitaxial layers on the crystal end surfaces. The crucible temperature was checked with the optical pyrometer.

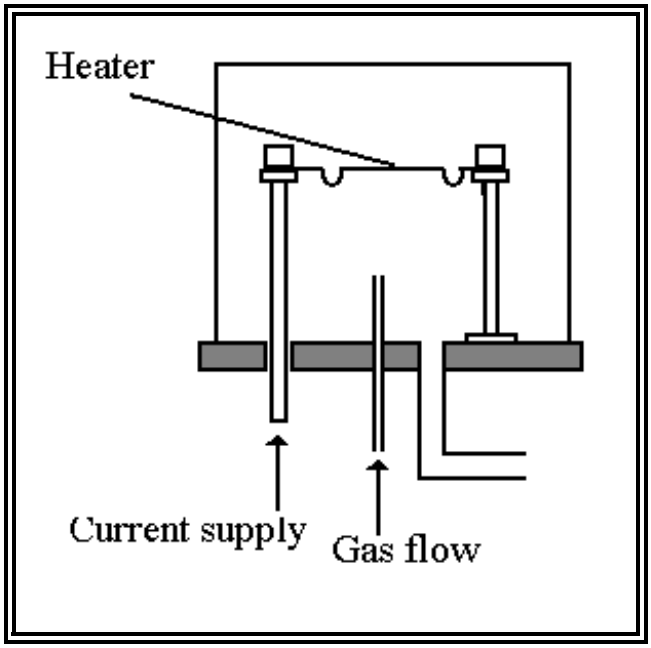

Fig.1.3.1. The vacuum chamber for the short time annealing

10/14/04

In charge *Date* *Signature*

POf *S. Sljusarenko, Ph.D*

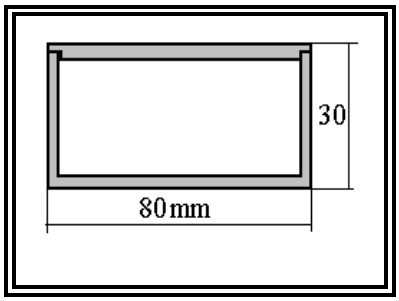

Fig.1.3.2. The crucible for the annealing

On the Fig.5 it is shown the time-temperature regime of annealing. Hear T_{an} – is the annealing temperature, and $\delta T=t_2 - t_1$ – is the time of annealing. The time constant depends on the masses of inner equipment of furnace (thermal shields, heater) and on electrical power.

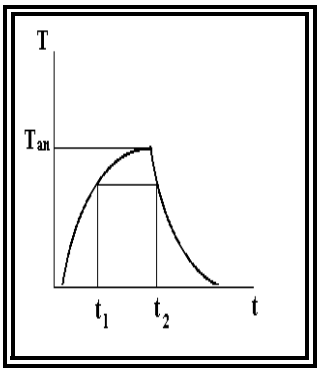

Fig. 1.3.3. The time-temperature regime of annealing

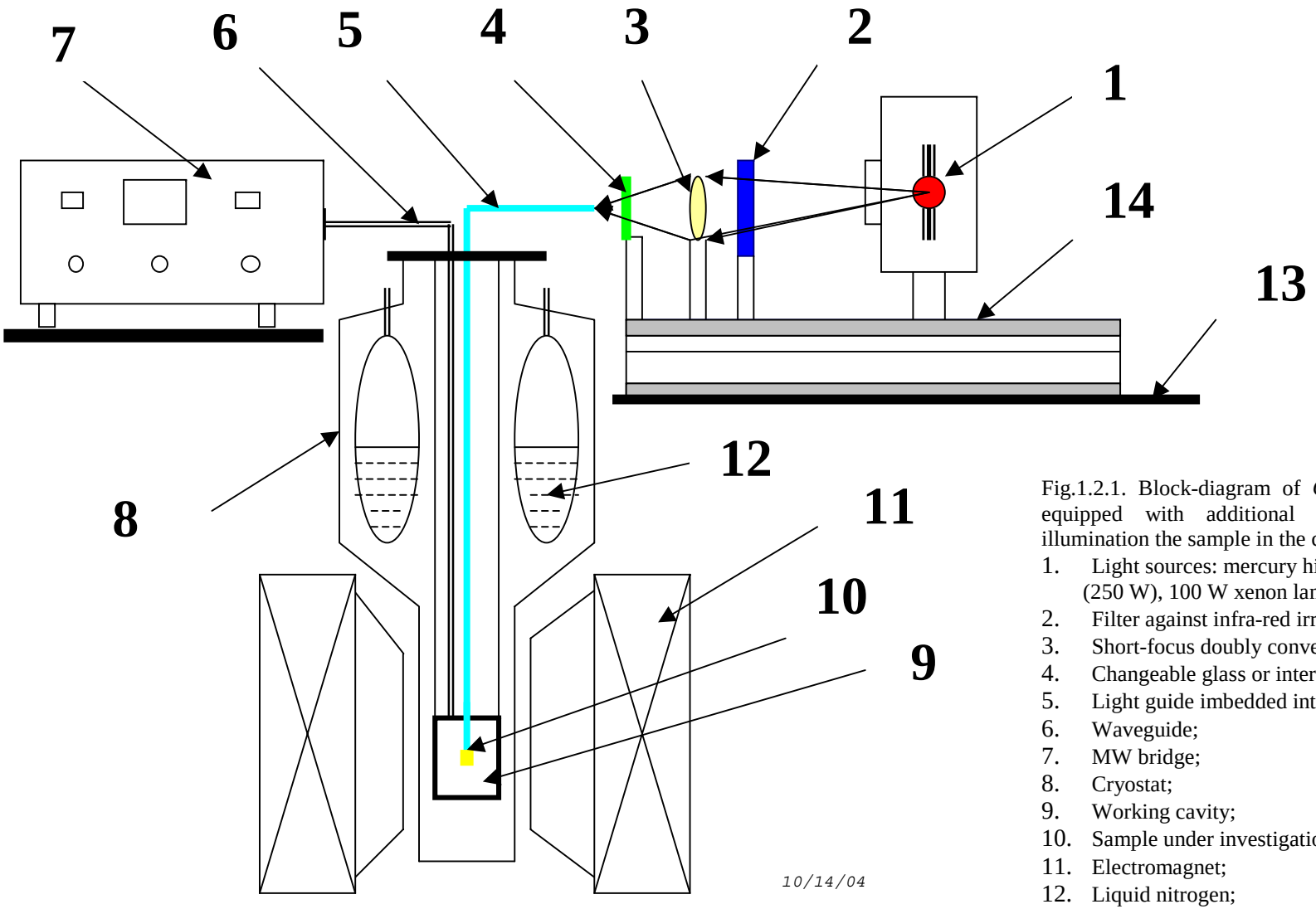

Fig.1.2.1. Block-diagram of *Q*-band EPR spectrometer equipped with additional optical arrangement for illumination the sample in the cavity.

1. Light sources: mercury high-pressure vapour lamp (250 W), 100 W xenon lamp;
2. Filter against infra-red irradiation
3. Short-focus doubly convex quartz lens;
4. Changeable glass or interference filter
5. Light guide imbedded into airproof shell
6. Waveguide;
7. MW bridge;
8. Cryostat;
9. Working cavity;
10. Sample under investigation;
11. Electromagnet;
12. Liquid nitrogen;
13. Work table;
14. Optical rail.

In charge *Date* *Signature*

POf *L. Taranenko, Ph.D*

1.4. Analysis and processing of experimental EPR data.

EPR parameters of the paramagnetic centers identified in s.-i. and n-type 4H SiC samples in the dark are collected in the table 1.4.1

Table 1.4.1. EPR parameters of paramagnetic centers identified in s.-i. and n-type 4H SiC samples in the dark.

Center	**S**	**I**	**$g_{\|}$**	**$g_{\perp}$**	**ΔH_{pp} G**	**$A_{\|}$, G**	**$A_{\perp}$, G**	**D, GHz**	**ΔT K**
B_C	1/2	3/2	2.0063	2.0046		2.0	0.9		4.2 - 77
B_h	1/2	3/2	2.0019	2.0070		2.0	1.2		4.2 - 77
N_C.	1/2	1	2.0043(1)	2.0013(1)	2.7	18.2	18.2		4.2 -77
$ND1_h$	1/2		2.0063(1)	2.0006(1)	2.5				4.2 - 54
$\boldsymbol{I_S^N}$	1/2		2.0067	2.0012					60-77
X_h	1/2	1/2	2.0025	2.0044(1)					4.2 - 77
X_C	1/2	1/2	2.0028	2.0043(1)					77 - 40
X_C	1/2	1/2							40 – 4.2
R	1/2		2.0025	2.0025					4.2 -77
$\boldsymbol{V_c^{3+}}$	1	7/2	1.959(5)	1.958(5)		64(1)	65(1.5)	2.65(5)	4.2 - 77
$\boldsymbol{V_h^{3+}}$	1	7/2	1.962(8)	1.958(8)		63(1)	68(1.5)	10.5(1)	4.2 - 77
Mn^{2+}	$3d^5(^6S_{5/2})$	5/2	2.000 (1)		70	106(2)	106(2)		4.2 - 77

As was seen from Table 1.1.1 –1.1.3, unannealed s.-i. samples revealed a broad EPR line labeled R from the defect which is vanished after annealing of the sample up to 1400^0 C. The g - factor of R defect with S=1/2 is in agreement with that of the signal from carbon-related surface defects (g = 2.0025 isotropic in 4H SiC) which has been studied in [1].

Vanadium doped PVT 4H SiC samples besides I_R line revealed the EPR spectra of vanadium in the $V^{3+}(3d^2)$ charge state (S = 1, I = 7/2) from the cubic and hexagonal sites in the temperature interval from 4.2 to 77 K in the dark.

The two hyperfine octets arising from cubic site V taken at 4.2 K and 37 GHz for $\boldsymbol{H} \parallel \boldsymbol{c}$ are shown in Fig. 1.4.1. The parameters of the spin Hamiltonian obtained from an analysis of the angular dependence of the EPR spectra for a rotation of the magnetic field in the $(11\bar{2}0)$ plane, listed in Table 1.4.1, are very similar to those obtained in [2] at 9 GHz. The signs of the fine structure parameters D were determined to be positive for the two V spectra from the difference in the intensity of the low and high field resonance transitions which, as seen in Fig. 1.4.1, are enhanced by raising the frequency and lowering the temperature to 4.2 K.

Only one 4H SiC Q0407-1 s.-i. sample and 6H SiC E 1062-10 s.-i. sample with vanadium concentration of $1.3x10^{16}$ and $3x10^{15}$ respectively reveal EPR spectra of boron in the dark with unresolved hyperfine structure from hexagonal and cubic site having C_{3V} symmetry at temperatures higher than 50 K [3].

EPR investigations of undoped HPSI 4H SiC samples were shown that the position of the Fermi level in the dark in this samples is determined by energy level of the X center.

At 77 K two EPR lines, X_h and X_c, have axially symmetric g-factors, isotropic width and correspond to the two inequivalent sites of the defect center with S=1/2. When the temperature decrease up to 40 K the transformation of one single line X_c into six EPR lines is occured showing that the symmetry of EPR spectrum is changed from axial C_{3v} to monoclinic symmetry for the defect residing cubic site. The behavior of the X defect EPR spectrum is typically for the center with Jahn-Teller distortion when degeneracy of three nearest neighbours C (Si) of the defect about c-axis at low temperature could be removed by Jahn-Teller distortion. Unfortunately, the ligand hyperfine structure (HFS) was not detectable in our spectrum due to the small concentration of the defect, estimated to be about $5 \cdot 10^{14} cm^{-3}$.

In addition to X defect some HPSI 4H SiC reveal EPR spectra of vanadium in the $V^{3+}(3d^2)$ charge state (S = 1, I = 7/2) from the cubic and hexagonal sites in the temperature interval from 4.2 to 77 K and EPR spectrum due to Mn^{2+}

(I= 5/2, S=5/2) in the dark.

As was seen from Table 1.4.2, the parameters of Mn^{2+} EPR spectrum observed in s.-i. 4H SiC samples are in agreement with those obtained for Mn^{2+} in 6H SiC samples by S. Greulich-Weber and J.-M. Spaeth [4] and was attributed to the Mn^{2+} with electron configurations $3d^5$. Based on the large hyperfine interaction of A = 96.4 G the Mn^{2+} was assigned with the interstitials localized in the hexagonal site. Only the central hyperfine sextet from Mn^{2+} with g = 2.003 was observed in EPR spectrum. The fine structure lines are broadened beyond detection probably due to random internal strains. EPR spectrum of Mn^{2+} is also observed by P.G.Baranov in GaN and has been attributed to Mn^{2+} in the $3d^5(^6S_{5/2})$ state [5].

Table 1.4.2. Parameters of the Mn^{2+} EPR spectrum in 6H SiC, GaN and 4H SiC.

Sample	**T, K**	**g**	**$A_{\|\|}$, G**	**$A_{\perp}$**	**D, G**	**ν, GHz**	
6H SiC	5	2.003±0.001	100.66G (270.1 MHz)	97.2G (272.6MHz)	88.8	9.17	[4]
GaN		1.999±0.001	66.5 G	66.5 G	228	9.23	[5]
4H SiC BH0429-12	77	2.000±0.001	106±2 ΔH_{pp}=70G	106±2 ΔH_{pp}=70G		37	
ZnO	4	2.0012±0.001	70.3	70.3	- 224	9	[6]

ΔH_{pp} - the width of the hyperfine line.

The parameters of Mn^{2+} in ZnO is also shown in Table 14.2, which has the same hexagonal wurzite structure and closely physical parameters. As was seen from Table 1.4.2, a good correspondence is observed between parameters of Mn^{2+} in ZnO, SiC and GaN crystals.

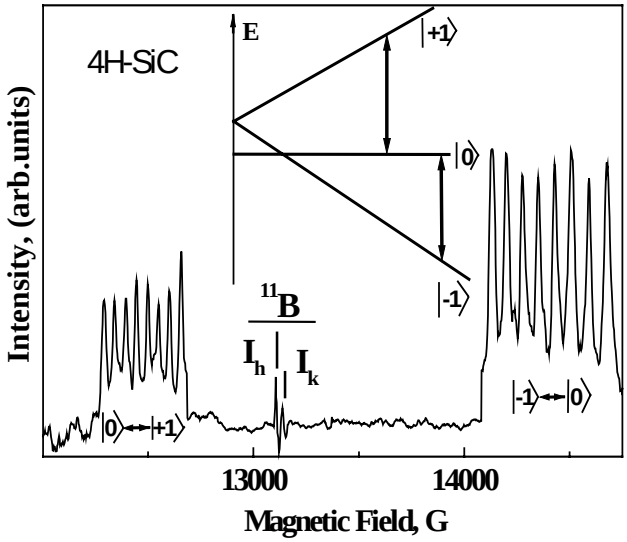

Fig. 1.4.1. Vanadium $V^{3+}(3d^2)$ EPR spectrum in s.-i. 4H-SiC measured at T = 4.2 K, 37 GHz and **B** ‖ **c**. The two hyperfine octets belong to the $V^{3+}(3d^2)$ cubic site. The energy level scheme for a triplet system in a static magnetic field is shown for D> 0.

The EPR spectra parameters of two donor paramagnetic states of nitrogen and a native defect ND1 which have been resolved in n-type mid n-type 4H SiC bulk material at 9.6 and 140 GHz in the temperature range of 4.2 K to 77 K are collected in Table 1.4.1. The ND1 defect has an axially symmetric g-factor, isotropic width and corresponds to a defect center with S = 1/2. The native defect ND1with the same EPR parameters on the quasi cubic and hexagonal positions has been previously observed in the 4H SiC epilayers with a deviation from stoichiometry towards carbon [7]. The weak EPR signal from the defect on the quasi cubic position $ND1_c$ is also shown in Fig.1. 1.6.

Both the nitrogen and $ND1_h$ EPR spectrum is accompanied by two satellites due to the ligand hyperfine structure (HFS) as indicated by arrows in Fig.1. As was seen from Table 1.4.2, the intensity of the satellites is about of (2.2 ± 0.3)% of both the nitrogen and $ND1_h$-line. The statistical prediction for the intensity of one hyperfine line with respect to the central line is 0.55 % for one ^{13}C nucleus with natural abundance of 1.1% and I = 1/2. Therefore these satellites could be attributed to the HFS due to the interaction between the electron spin and the nuclear spin of four equivalent ^{13}C atoms in the nearest neighbor shell of a paramagnetic center.

Table 1.4.3. Calculated and measured relative intensities of ^{13}C ligand hyperfine lines.

Intensity ratio	Theory (4 x ^{13}C)	Experiment 9.6 GHz	Experiment 140 GHz
a/A	0.022	0.023 ± 0.003	0.020 ± 0.002
(b+a)/B	0.044		0.043 ± 0.005
(b+c)/B	0.044		0.050 ± 0.006
c/C	0.022	0.019 ± 0.002	0.019 ± 0.002
d/$ND1_h$	0.022	0.027 ± 0.004	0.025 ± 0.004

As was seen from Fig. 1.1.5, in D-band the low field ^{13}C satellite line is overlapped with the related $ND1_h$ EPR line due to a small shift in g-factor caused by the isotopic effect, and the intensity of the two inner ^{13}C satellite lines labeled (a+b) and (b+c) surrounding the central nitrogen triplet line B are about double that of the outer ^{13}C satellite line intensities due to the overlap of two of them.

Table 1.4.4. collects the g-factors and values of the HF interaction with ^{13}C nucleus obtained for ND1 defect and the nitrogen donor from EPR and ENDOR measurements.

As was seen from Table 1.4.4, the ^{13}C interaction constant A is isotropic and has the same value both for the nitrogen donor and the defect line, showing that electron density is equally distributed over the four C atoms surrounding the nitrogen and defect that occupy a silicon site in the lattice. This conclusion is consistent with that made in [8] that the main part of the spin density of nitrogen in 4H SiC, in contrast to 6H SiC, is located in the Si sublattice. The much smaller isotropic values of the HF interaction with ^{13}C nucleus obtained for the nitrogen donor from ENDOR measurements in [9] should be assigned to the next neighbor shells.

Table 1.4.4. EPR parameters of nitrogen donor and ND1 defect in 4H SiC.

Cent.	S	$g_{\parallel}$	$g_{\perp}$	Δg	A ^{14}N [MHz]	A ^{13}C [MHz] EPR	A ^{13}C [MHz] ENDOR	A ^{29}Si [MHz] ENDOR
N_c	1/2	2.0043	2.0013	0.0030	51	51	5.02	$A_{\parallel}$=9.06 $A_{\perp}$=5.28
N_h	1/2	2.0055	2.0010	0.0045	$A_{\parallel}$=3.06 $A_{\perp}$=2.82		$A_{\parallel}$ = 5.86	$A_{\parallel}$=8.66
$ND1_h$	1/2	2.0063	2.0006	0.0057	ΔH_{pp} = 2.5G	51		
$ND1_c$	1/2	2.0058	2.0033	0.0025	ΔH_{pp} = 2.5G			

The fact that the value of the ^{13}C isotropic HF interaction constant for nitrogen on a quasi-cubic site was found to be an order of magnitude larger than those determined from ^{29}Si and ^{13}C ENDOR spectra enabled us to conclude that nitrogen in 4H SiC occupies the silicon site in the lattice but not the carbon site as was previously accepted [9].

References.

[1]. P.J. Macfarlane, M.E. Zvanut, J. Vac. Sci. Technol. B **17** (4), 1627, 1999.
[2]. J. Schneider et al., Appl. Phys. Lett. 56 (1990) 1184.
[3]. S. Greulich - Weber, F. Feege, E.N. Kalabukhova, S.N. Lukin, J.-M. Spaeth, F.J. Adrian Semicond. Sci. Techn. 13,
[4] M.Feege, S. Greulich-Weber, J.-M. Spaeth //Observation of an interstitial manganese impurity in 6H SiC// Semicond. Sci. Technol. **8**, pp 1620-1625, 1993
[5] P.G.Baranov, I.V. Ilyin, E.N. Mokhov, A.D. Roenkov // Identification of manganese trace impurity in GaN crystals by electron paramagnetic resonance // Semicond. Sci. Technol. **11**, pp 1843-1846, 1996
[6] A. Hausmann Solid State Commun. **6,** 457, 1968.
[7] E.N. Kalabukhova, S.N. Lukin, B.D. Shanina, Yu.A. Vodakov, A.A. Lepneva, E.N. Mokhov: Spring. Proceed. Phys. Vol.71 (1992), p. 703.
[8] A.v. Duijn-Arnold, R. Zondervan, J. Schmidt, P.G. Baranov, E.N. Mokhov: Phys. Rev. Vol. 64 (2001), p. 085206
[9] S. Greulich-Weber: Phys. Stat. Sol. (a) Vol. 162 (1997), p. 95.

-

2.1. 2.2. Investigation of TR of non equilibrium charge carriers at defects and impurities by photo EPR method including photo-excitation and photo-quenching method in s.-i. SiC before and after annealing the samples in the temperature interval from 1400 C to 1800 C at 77 K.

The results of photo testing of the s.-i. and n-type, mid n-type 4H SiC samples are collected in Table 2.1.1.

Nitrogen, with an 0/+ energy level at E_C - 0.054 eV, E_C - 0.090 eV [1] , and boron, with an (-/0) energy levels near E_V + 0.35 eV [2],[7] are the major contaminants in SiC and both are paramagnetic in the dark in n-type and p-type SiC. However, in s.-i. samples they are in non paramagnetic state in the dark due to the pinning of the Fermi level by mid-gap levels. From the other side the creation of mid-gap levels in SiC crystals forces the Fermi level to move towards the middle of the band gap, and, as a result, the capture of photo created carriers becomes more and more efficient both for shallow donors and acceptors which can then play an important role in the recombination process.

Thus, the excitation of the s.-i. samples with the light gives rise to the transition of them from a diamagnetic ground state into observable paramagnetic state depending from the location of the quasi Fermi level at given temperature.

It was established that in HPSI 4H SiC samples under investigation Fermi level was pinned at X defect level in the dark. The situation was changed when the samples were photo excited. The photo excitation with above band gap light at 77 K give rise to the quenching of the X-lines and appearance of the boron, nitrogen, defect EPR lines depending on the location of the quasi Fermi level in the sample at given temperature.

Excitation of the first type of the samples with band gap light at 77 K resulted in the neutralization of the shallow donors and acceptors $N^+ + B^- + e + h \rightarrow N^0 + B^0$ and as result the EPR signals from nitrogen on cubic site, I_k^N, which is easily recognized by the characteristic three line hyperfine pattern and g = 2.0013 and boron with unresolved hyperfine structure on the cubic I_C^B and hexagonal site I_h^B, having C_{3V} symmetry at temperatures higher than 50 K, are appeared in EPR spectrum, see Fig. 2.1.1.

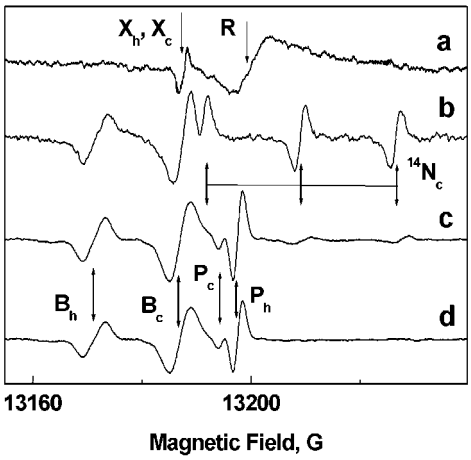

Fig.2.1.1. EPR spectrum measured in a series of HPSI 4H SiC samples in the dark (a) and under illumination with band gap light (b-d). **B⊥c.** ν = 37 GHz, T = 77K. B_c, B_h, ^{14}N - EPR spectrum of boron ^{11}B and nitrogen.

The photo excitation EPR spectrum of second type of the samples consists of EPR signals of boron and nitrogen of small intensity and two additional lines due to the defect labeled P in two inequivalent sites, see Fig. 2.1.1.c.

The third sample revealed only EPR spectrum of boron and the P defect, without the nitrogen spectrum, see Fig. 2.1.1d.

The different behavior of the samples under band gap excitation demonstrates the different position of the quasi Fermi levels in the band gap at given temperature in the HPSI 4H SiC samples under investigations.

As the temperature increase from 77 K to 140 K the quasi-Fermi levels for electrons, ϕ_n, and holes, ϕ_p are moving towards the middle of the band gap, as a result, the capture of free carriers becomes more and more efficient on the deep levels which become paramagnetic.

On other hand as the temperature goes down to the 4.2 K, the quasi-Fermi levels for electrons ϕ_n, and holes, ϕ_p, fall to the edge of the conduction and valence band respectively. As result, the population of the paramagnetic centers with different energy levels is changed and the transition of the defect centers with shallow energy levels from a diamagnetic ground state into observable paramagnetic state occurs.

Particularly, the intensity ratio of boron EPR lines corresponding to the quasicubic and hexagonal sites at 77 K $I_B^k : I_B^h = 2$ is reversed to 0.5 at 50 K and the EPR line from defect center labeled ND1 appeared in EPR spectrum at 50 K.

-

The effect of band gap illumination on the EPR spectra of the s.-i. sample at the lower temperatures is shown in Fig. 2.1.2. An additional EPR line labeled ND1 appeared in the excitation EPR spectrum of the first type of s.-i. sample at 50 K. The parameters of this line, $g_{||} = 2.0063$, $g_{\perp} = 2.0006$, coincided with those found for a native defect located on an hexagonal site in EL 4H SiC grown off stoichiometry with excess carbon [3].

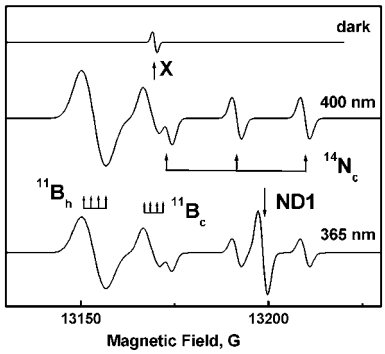

Fig. 2. 1.2. EPR spectrum of s.i. 4H SiC sample measured at 37 GHz and 50 K in the dark and under illumination with the light of different photon energies. **B**⊥**c**. B_c, B_h -EPR spectrum of boron ^{11}B.

It should be noted that a comparison of the integral intensities of the boron and nitrogen EPR spectra, which are proportional to the concentrations of the paramagnetic centers shows the large difference between the amount of light–induced electrons (the concentration of nitrogen) and holes (the concentration of boron) in the s. - i. sample which was not annealed**.** This difference could be caused by existence of a large number of the structural defects in s. - i. material which also capture electrons. Indeed as was shown in Fig. 2.1.3, the 1400^0C heat treatment of the samples leads to increase of the light–induced electron amount captured by nitrogen and P center and as result the light-induced amplitudes of the donor and acceptor EPR signals become comparable.

The fact that the integral intensity, which is proportional to the number of paramagnetic centers, of the cubic site boron EPR line is higher than that for hexagonal site boron, $I_B^k : I_B^h = 1.3$, at 77 K in three types of the samples make it possible to conclude that the hexagonal site boron is shallower than cubic site boron and the location of quasi-Fermi level should be above the level in the band gap of boron on the hexagonal site for s.–i. 4H SiC at 77 K. When the temperature is lowered the ratio of the photo-excited EPR line intensities responsible for boron on the cubic and hexagonal sites, $I_B^k : I_B^h$, is reversed from that at 77K, showing that the quasi-Fermi level moving down to the valence band and concentration of boron in the hexagonal site is higher than that on the cubic site.

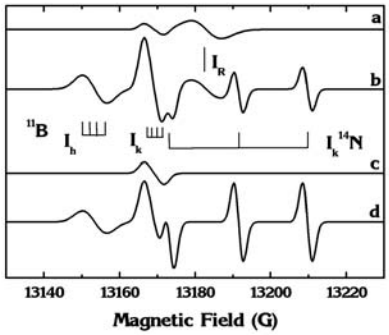

Fig. 2. 1.3. The photo excitation EPR spectrum of semi - insulating 4H-SiC measured at ν = 37 GHz, T = 77 K before (a, b) and after (c, d) annealing at T = 1400^0C. a, c - dark, b, d - excitation with UV light.

The principle feature of s.-i. material is that the lifetime of the electrons and holes captured on the intrinsic defect and impurity levels is very long of about 10-14 hours and more at low temperature. The metastable state of the photosensitive intrinsic defects and impurities indicate that at low temperature the recombination rate of the photo-created carriers is very small. This phenomena is observed in many semiconductor structures and called persistent photoconductivity [4].

Fig. 2.1.4 shows the photo excitation and photo quenching of P center in the third type of HPSI 4H SiC sample. P is quenched at about 2.1 eV making it possible to determine the energy level for P at $E_C - (1.15 \pm 0.06)$ eV. The concentration of the P defect estimated from the integrated intensity of EPR signal is about $2 \cdot 10^{15}$cm^{-3}.

-

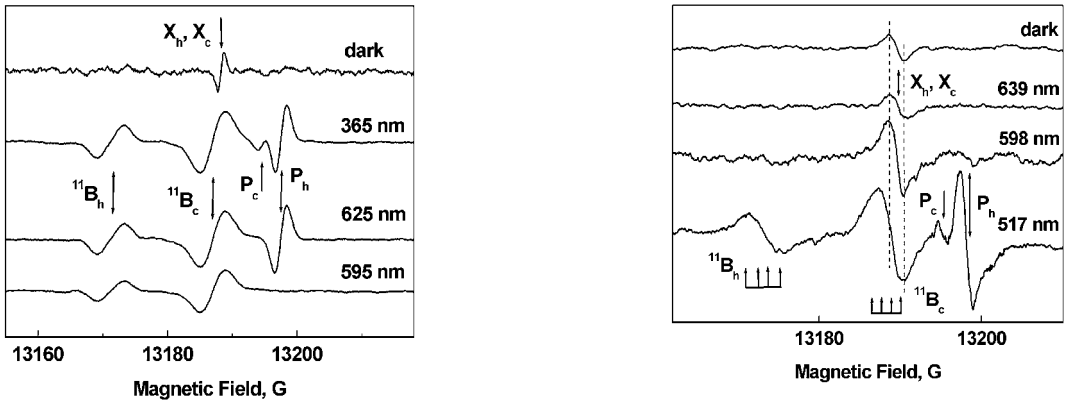

a b

Fig.2.1.4. Behavior of the EPR spectrum of s.i. 4H SiC sample under illumination with the light of different photon energies. **B⊥c.** ν = 37 GHz, T = 7 7K. $T_{annel.}$=1800^{0}C. B_c, B_h -EPR spectrum of boron ^{11}B.

On the other hand, as is seen in Fig. 2.1.4 b, the X center appears to be photosensitive and when the sample is illuminated at about 2.11 eV (598nm) the intensity of the X line begins to decrease, while boron EPR lines appear and increase until the photon energy reaches 2.4 eV. The transformation of the X line into the cubic boron line in this energy range is clearly seen in Fig. 2b due to the difference in their width line. The photo quenching of the X center is accompanied by the photo excitation of the two P center lines, which occur in the EPR spectrum with approximately the same photon energy threshold as the X center at about 2.1 ± 0.06 eV. Uncertainty in energy determination of about ≤ 0.06 eV does not allow to distinguish X and P defect levels. Taking into account that P was not observed in the dark, the position of the Fermi level and energy level of X center should be below the energy level of P defect. The situation similar to that which was observed for nitrogen (^{14}N) in 4H and 6H SiC. In spite of a small difference between the energy level of ^{14}N in cubic and hexagonal (h) sites (0.05 eV) appearance and intensity of EPR signal from shallow ^{14}N in h sites strongly depends from the location of the Fermi level [5].

The correlation observed between the decay and rise in intensity of the signals for X and P at approximately the same energy could be explained by a charge transfer process between them. The electrons excited by the light from the X center could be captured on the energy level of the P center via the conduction band.

As seen in Fig. 2.1.2, the ND1 defect occurs inside the EPR spectrum of nitrogen in the s.i. sample when illuminated by light with an energy threshold at about hν = 3.19eV (365 nm). Taking the threshold energy as the energetic distance of the ND1 defect from the valence band, one can estimate the position of the energy level of ND1 as $\Delta E = \Delta E_g$ - 3.19 eV = E_C – 0.07 eV indicating that the defect originates from a shallow donor state with an ionization energy between the cubic and hexagonal nitrogen energies.

The illumination with above bandgap UV light of the vanadium doped s.-i. samples gives rise to the appearance of EPR lines due to the boron acceptor on hexagonal and cubic sites in EPR spectrum of vanadium. This shows that vanadium previously considered to be non-paramagnetic [6], can also be in a paramagnetic state in p-type SiC. At the same time, the vanadium spectrum itself does not change with illumination.

2.3. Preparation and annealing of the s.-i. SiC samples in the temperature interval from 1400^0 C to 1800^0 C.

The s.-i. samples supplied by AFRL/MLPS laboratory have been annealed at 1400^{0}C and 1800^{0}C in inert atmosphere. .

2.4. Analysis and processing of experimental EPR data. Comparison of the data obtained by EPR with that obtained by electrical and optical methods in AFRL/MLPS laboratory.

It was established that in all HPSI 4H SiC samples under investigation Fermi level was pinned at X defect level located in the upper half of the band gap in the dark. All others impurities and defects such as nitrogen, boron and P ND1 intrinsic defects are in a non-EPR active state. Excitation of the samples with the light gives rise to the transition of them from a diamagnetic ground state into observable paramagnetic state depending from the location of the quasi Fermi level at given temperature. Parameters of EPR spectra and energy levels of the photosensitive intrinsic defects observed in HPSI 4H SiC are collected in the Table 2.4.1. As was seen from Table 2.4.1, the intrinsic defects are donor like and located in the upper half of the band gap. All defects are temperature stable at least up to 1800 ^{0}C, indicating that the defects are not vacancy-related complexes since these are not stable at 1800 ^{0}C.

Identification of the defects using ligand hyperfine structure (HFS) is constrained due to weak intensity of their EPR signals appeared in EPR spectrum of s.-i. 4H SiC sample under illumination of the sample with the light.

It should be notice, that in as-grown SiC sample the intensity of the EPR lines from intrinsic defects usually of one order weaker than that in irradiated SiC and often immersed in the noise level. This fact is strongly hampered EPR identification of the intrinsic defects using their ligand HFS especially in the case when the defect resides the silicon site since there is better chance of detecting the HFS of ^{29}Si (I=1/2, 4.7% natural abundance) than that of ^{13}C (I=1/2, 1.11 % natural abundance).

Table 2.4.1. Parameters of EPR spectra and energy levels of the photosensitive intrinsic defects observed in HPSI 4H SiC.

Center	X_h	X_c	P_h	P_c	$ND1_h$	$ND1_C$	EI5 [3]
$g_{\|\|}$	2.0025	2.0028	2.0048	2.0030	2.0063	2.0058	2.0032
$g_{\perp}$	2.0044	2.0043	2.00365	2.00365	2.0006	2.0033	2.0048
Symmetry	C_{3V}	C_{3V}	C_{3V}	T_d	C_{3V}	C_{3V}	C_{3V}
ΔT, K	4.2 - 110	40 - 110	50 - 107	50 - 77	4.2 -50	4.2 -50	25 - 140
Symmetry		D_{2d}					
ΔT, K		40-4.2					
$E_C - E_i$ [eV]	<1.15	<1.15	1.15	1.15	0.07	0.07	1.79

An attempt to identify P center using its ligand HFS has been undertaken on n-type 4H SiC epilayer (EL) grown in the presence of Sc in the vapour phase enhancing the carbonization of 4H SiC. In this sample P EPR signal is resolved at 140 GHz in EPR spectrum of nitrogen and ND1 defect at 4.2 K in the dark.

EPR spectra of the defects and nitrogen are accompanied with the satellite lines. As was seen from Fig. 4, only outer components of each satellite pairs surrounding the defects could be resolved while inners are hidden inside the EPR spectra of nitrogen and defects. The satellite lines accompanied nitrogen EPR spectrum labeled a, b, c are appeared in pairs in EPR spectrum. For $\mathbf{B_0}$ parallel to the c-axis two satellite lines labeled g and f at high magnetic field related to the P center and satellite line labeled e at low magnetic field related to ND1 defect are illustrated in Fig. 2.4.1.

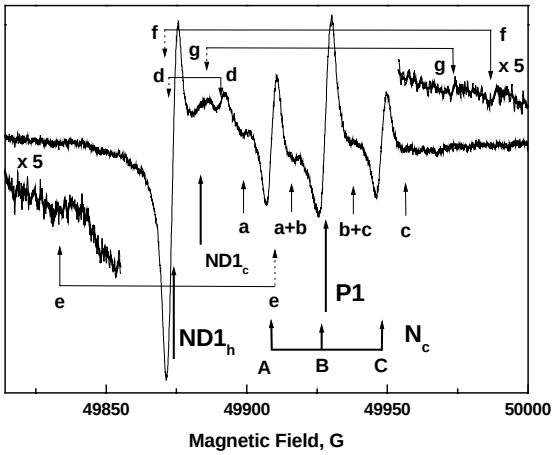

Fig.2.4.1. EPR spectrum of n-type 4H SiC EL grown in the presence of Sc in the vapour phase. a, b, c - ^{13}C satellites related to nitrogen (N_c), g, f - ^{13}C satellites related to P center. d, e ^{13}C satellites related to ND-1 defect N_c, N_h – EPR spectrum of the nitrogen in cubic and hexagonal sites. T =4.2 K, ν = 140 GHz. $\mathbf{B_0}||\mathbf{c}$.

As was seen from Table 2.4.2, the intensity ratio between central and satellite line g is about 0.005. The statistical prediction for the intensity of one hyperfine line with respect to the central line is 0.55 % for one ^{13}C nucleus with natural abundance of 1.1% and I = 1/2. Therefore this satellite line is believed to be the HFS due to the interaction between the electron spin and the nuclear spin of one among the four ^{13}C atoms in the nearest neighbor shell of a paramagnetic P center indicating that P center is related to the defect occupying a silicon site in the lattice. At this direction of magnetic field the interaction with other three carbon atoms C(2,3,4) (see Fig. 2.4.2) are equivalent and give rise to the same lines labeled f with triple intensity compared that of the satellite line labeled g. This indicates that one distinguishes between axial ligands (direction of the bond along **c**-axis) and basal ligands (the angle between the direction of the bond and the c-axis is a tetraeder angle).

Table 2.4.2. Calculated and measured relative intensities of ^{13}C ligand hyperfine lines related to nitrogen, ND1 and P intrinsic defects.

Intensity ratio	Theory (1,2,3,4 x^{13}C)	Exper. 140 GHz $\mathbf{B_0} \| \mathbf{c}$	Exper. 140 GHz $\mathbf{B_0} \perp \mathbf{c}$	Exper. 9.6 GHz $\mathbf{B_0} \| \mathbf{c}$ [4]	Exper. 9.6 GHz $\mathbf{B_0} \perp \mathbf{c}$ [4]
a/A	0.022	0.020± 0.002	0.020± 0.002	0.019± 0.003	0.018± 0.003
(b+a)/B	0.044	0.043± 0.005			
(b+c)/B	0.044	0.050± 0.006			
c/C	0.022	0.019± 0.003		0.019± 0.002	0.019± 0.002
d/ND1$_h$	0.022	0.025 ± 0.004		0.027 ± 0.004	
e/ND1$_h$	0.0055	0.0055± 0.001	0.0055± 0.001		
g/P$_h$	0.0055	0.0055± 0.001	0.0055± 0.0015		
f/P$_h$	0.0165	0.0165± 0.005			
h/P$_h$	0.011		0.011 ± 0.005		

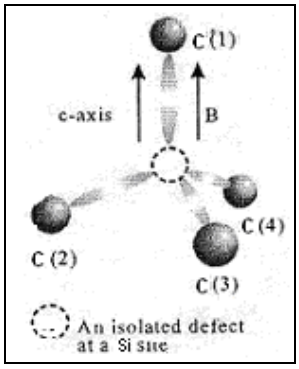

Fig. 2.4.2. An isolated defect Si site with the magnetic field parallel to the c axis. The expected symmetries of the hyperfine tensors representing the interaction with C(1) and C(2,3,4) are C_{3V} and C_{1h}, respectively.

As indicated in Fig. 2.4.3, for $\mathbf{B_0} \perp \mathbf{c}$ the P center is also accompanied by two satellite lines. One line with the same splitting as for the satellite line labeled g at $\mathbf{B_0} \| \mathbf{c}$ could be attributed to the axial ligands while other having approximately double intensity compared that of the satellite line g could be attributed to the interaction with the C(3) and C(4) atoms which become equivalent with respect to the direction of the magnetic field. Calculated and measured relative intensities of ^{13}C ligand HF lines related to nitrogen, ND1 and P intrinsic defects are listed in Table 2.4.2.

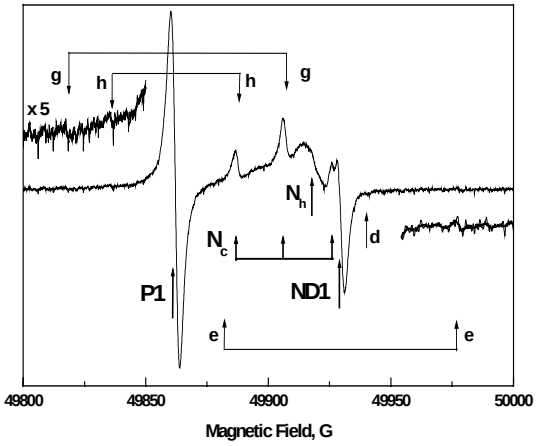

Fig. 2.4.3. EPR spectrum of n-type 4H SiC EL grown in the presence of Sc in the vapour phase. g, h - ^{13}C satellite lines related to P center. d, e ^{13}C satellite lines related to ND-1 defect N_c, N_h – EPR spectrum of the nitrogen in cubic and hexagonal sites. T =4.2 K, ν = 140 GHz. $\mathbf{H_0} \perp \mathbf{c}$.

-

The second important intrinsic defect ND-1 with $g_{\|}$ = 2.0063, $g_{\perp}$ = 2.0006 and electron spin S = 1/2, which always presents in C-rich n-type 4H SiC is accompanied by satellites labeled e. In addition to HF interaction with four next nearest ^{13}C nucleus which was detected for ND-1 defect at 9 GHz, the satellite line e with intensity ratio between central line and satellite line of about 0.005 has been detected in EPR spectrum of ND1 defect at 140 GHz with the same value of splitting for $\mathbf{B_0} \perp \mathbf{c}$ and $\mathbf{B_0} \| \mathbf{c}$ in 4H SiC EL grown in the presence of Sc (see Fig. 2.4.1, 2.4.3). Observed HF interactions with the four next nearest ^{13}C nucleus proved that the ND-1 defect resides Si site whereas the presence of the hyperfine interaction with one ^{13}C atom with largest HF splitting than that for the four next nearest ^{13}C nucleus indicates that there is a central HF interaction with one ^{13}C. This fact strongly suggests that the ND1 defect involves a C atom occupying a Si site, i.e., a C_{Si} antisite.
The results of the analysis of hyperfine interaction are given in Table 2.4.3.

Table 2.4.3. Results of ligand HFS analysis of nitrogen and ND1, P intrinsic defects.

Cent.	**S**	**$g_{\|}$**	**$g_{\perp}$**	**A, G ^{14}N**	**A, G (4x^{13}C)**	**A, G (1x^{13}C)**	**A, G (3x^{13}C)**	**A, G (2x^{13}C)**	**E_i [eV]**	**Model**
N_c	1/2	2.0043	2.0013	18.2	18				0.087	N_{Si}
$ND1_h$	1/2	2.0063	2.0006	ΔH_{pp} = 2.5	18	$A_{\|}$= $A_{\perp}$= 78			0.07	C_{Si}^{-}
P_h	1/2	2.0048	2.0030	ΔH_{pp} = 2.3		$A_{\|}$= $A_{\perp}$= 86	$A_{\|}$ = 120	$A_{\perp}$=54	1.15	V_{Si}^{3-}

Unfortunately, due to the weak intensity of the satellite lines which are not detectable at intermediate angles and severe overlapping of the one component of each satellite pairs with other EPR spectra, it was impossible to study of the angular dependencies of the ligand HF interaction and to determine the parameters of the hyperfine tensors. Moreover, as was shown in **Fig. ,** a small difference in g-factor of the central and satellite lines caused by isotopic effect should be also considered when measuring at high frequency, which gives rise to the addition uncertainty in determination of the hyperfine splitting for g, f, e, h satellite pairs. Therefore the HF splitting values listed in Table 2.4.3 should be considered as estimation data.

Considering that P defect is localized at $\Delta E = \Delta E_g - 2.11 = E_C - 1.15$ eV in the band gap and observed in n-type material along with the nitrogen EPR spectrum, the charge state +1 unlikely.

In accordance with the theoretical predictions made in [7, 8] possible identification of the donor-like monovacancies, located in the upper half of the band gap, with the low spin state S =1/2, are the carbon and silicon vacancies in the negative charge states –1 and –3 respectively. Hence the P center which is assigned to the silicon vacancy could be attributed to the V_{Si}^{3-} and photo quenching process for the P defect will be described by the following charge transitions

$$V_{Si}^{3-} - e^{-} \rightarrow V_{Si}^{2-}.$$

Comparing the EPR parameters for the X center with those for EI5 [9], which has been associated with the carbon vacancy in the positive charge state +1, in Table 2.4.1, we can suggest that the donor-like X center is related to the carbon vacancy in the negative charge state –1. The absence of the EPR signal from V_C^{+} in the dark and under photo excitation in our HPSI 4H SiC samples could be explained by the difference in location of the Fermi level and quasi Fermi levels in HPSI 4H SiC samples investigated in [9-11] and in present work., see Fig.2.1.4.

This suggestion is supported by the temperature behavior of the X defect residing the quasicubic site. As was shown in ***Fig.*** when the temperature decrease the transformation of one single line X_c into six EPR lines is occured showing that the symmetry of EPR spectrum is changed from axial C_{3v} to monoclinic symmetry for the defect residing quasicubic site. The behavior of the X defect EPR spectrum is typically for the center with Jahn-Teller distortion when degeneracy of three nearest neighbours C (Si) of the defect about **c**-axis at low temperature could be removed by Jahn-Teller distortion.

According to the single one-electron model, the electronic structure of a vacancy in a covalent solid is described by molecular orbitals constructed from four dangling bonds next to the vacancy. The defect molecular orbitals consist of the lowest a_1 one and a triply degenerate t_2 one, so a_1 can accommodate two electrons and t_2 six.

However, the crystal can usually gain energy by relaxing atoms next to the vacancy. Lowering the symmetry destroys the degeneracy of the t_2 orbital, provided that the energy gained by the overlapping dangling bonds overcomes the energy lost in distorting the lattice. This effect is called the Jahn-Teller distortion.

-

For a vacancy system, which is not subject to a the Jahn-Teller distortion, the exchange interactions can result in high-spin ground states. In fact, for Si vacancy in SiC the high spin ground state is more prefarably. As follows from theoretical prediction Si vacancy is generally T_d symmetry or close to that, less frequently a lower symmetry like $C_{3v.}$

On the other hand carbon vacancies in neutral or negative charge states are characterized by large Jahn-Teller distortion inward relaxations, resulting in breaking of the T_d symmetry towards D_{2d} symmetry [8]. In addition for the singly negative charge state it was found a significant difference between C vacancies at cubic and hexagonal lattice.

To explain the observed temperature transformation of EPR spectrum of X defect let us suppose that X defect has one unpaired electron. In this case the neutral state of the X defect has seven electrons and the ground state for undistorted tetrahedron $Si(C_4)$ or $C(Si_4)$ is threefold degenerate of T symmetry. For the defect residing the hexagonal site the unpaired electron is localized at the orbital parallel to the **c** axis and symmetry of the EPR spectrum does not change with increasing the temperature. For the defect residing the quasicubic site the unpaired spin occupies one of three others orbital perpendicular to the **c** axis at low temperature and the symmetry of the defect is low. At elevated temperature due to the thermally activated reorientation of the electron between three bonds about **c**-axis the symmetry of the defect EPR spectrum residing cubic site becomes higher (C_{3v}).

According to the resolved ligand hyperfine interactions in EPR spectrum of ND1 defect which exhibited strongest HF interaction with one ^{13}C atom than that with four next nearest ^{13}C it was concluded that there is a central HF interaction with one ^{13}C and ND1 defect involves a C atom occupying a Si site forming the carbon antisite C_{Si} which has the lowest formation energy in C-rich material [7].

On the other hand following the theoretical predictions made in [7] the carbon antisite exists only in the charge-neutral state and there is no experimental evidence to prove its presence in the band gap. Therefore the convincing identification of the carbon antisite would only be possible if ionization level and charge state of ND1 defect are found. As follows from photo EPR measurements the ND1 defect is a shallow donor with an ionization energy between the cubic and hexagonal nitrogen energies: $E_C - 0.07$ eV.

The position of the ionization level of ND1 defect could be also estimated from the comparison of the temperature behavior of nitrogen and ND1 EPR spectra.

Table 2.4.4 lists the temperature characteristics of the donor EPR spectra in 4H SiC epilayers samples with different degree of compensation varying from $2\cdot10^{18}cm^{-3}$ to $1\cdot10^{16}cm^{-3}$. With increasing degree of compensation the temperature interval of observation of ESR spectra of nitrogen on cubic sites shift toward higher temperatures, while the region where EPR line due to nitrogen on hexagonal site and ND1 defect are observed shift toward lower temperatures. This behavior can be explained with the following ratio.

Table 2.4.4. Temperature characteristics of the donor EPR spectra in 6H-, 4H SiC crystals with different degree of compensation.

Polytype	**E_D, meV**	**ΔT_i, K**	**(N_D-N_A), cm^{-3}**			
			$2\cdot10^{18}$	$8\cdot10^{17}$	$4\cdot10^{17}$	$1\cdot10^{16}$
6H SiC	120-150	ΔT_c	4.2 - 110	4.2 - 125	4.2 - 130	4.2 - 145
	85-80	ΔT_h	4.2 - 85	4.2 - 70	4.2 - 60	4.2 - 30
4H SiC	90	ΔT_c	4.2 -110	4.2 - 125	4.2 - 130	4.2 - 145
	40	ΔT_h	4.2 - 85	4.2 - 70	4.2 - 60	4.2 - 34
	40< E_D <90	ΔT_{ND1}		4.2 - 77 4H SiC:Sc	4.2 - 54 $T_{annel.}=1800^0C$	4.2 - 34 before annealing

The intensities of donor EPR lines decrease with increasing the temperature are apparently due to ionization of donors. The number of ionized donor electrons excited to the conduction band n_0 at low temperature could be described by [12]:

$$n_0 \approx \beta \cdot N_C \left[\frac{N_D - N_A}{N_A}\right] \exp\left(\frac{-E_D}{kT}\right) \qquad (2.4.1),$$

where N_C and β are the conduction band density of states and degeneracy, respectively, N_D and N_A are the donor and acceptor concentrations and E_D is the energy ionization of donors.

As follows from (2.4.1) the same number of excited electrons could be obtained with the different ratio of N_D/N_A at the different temperature. When the degree of compensation is rather large and N_D/N_A approaches unit the temperature of ionization in exponential must be higher to give the same number of excited electrons for nitrogen on cubic sites. For the shallow level of nitrogen on hexagonal site the two deeper levels of nitrogen on cubic sites play the role of acceptors. In this case when the ratio of $N_h/N_k \leq 1$ (the sample is lightly compensated $N_D/N_A > 1$) the temperature of ionization in exponential must be higher to give the same number of excited electrons than in the case of $N_h/N_k < 1$ (the sample is highly compensated, when $N_D/N_A \rightarrow 1$). Since the temperature behavior of the ND1 defect is

-

quite similar to that observed for the shallow nitrogen donor on hexagonal site the ND1 defect should be attributed to the donor with shallow level localized close to the level of nitrogen on hexagonal site.

Taking into account that the ND1 defect has axially symmetric g-factor and corresponds to the donor defect center with S = 1/2 it was concluded that ND1 defect is a carbon antisite in a single negative charge state.

Correlation between optical, electrical and EPR data.

The electrical and optical properties were found to correlate with the paramagnetic properties of the s.-i. samples. In the PL experiments, both sets of samples revealed spectra in the 0.95 eV region from the intra-3*d*-shell transitions of vanadium which show the polytype to be 4H [6]. In addition, as shown in Fig. 2.4.4, a broad band near 2.4 eV has been observed along with the typical near-bandedge sharp luminescence lines. For the first set of samples, which contains higher concentrations of V, the peak position of the 2.4 eV band is located at 2.43 eV. For the sample in which SIMS was unable to detect V, the peak shifts to 2.38 with a shoulder at about 2.14 eV, which is close to bandgap minus the activation energy of the P center

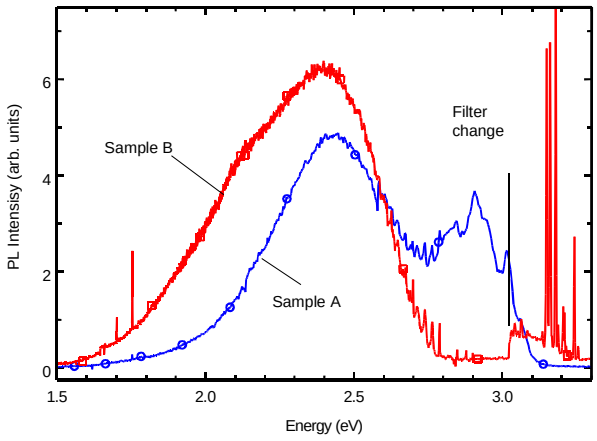

Fig. 2.4.4. PL spectra for two 4H-SiC samples. Sample A contains vanadium while V is undetectable by SIMS in sample B. The feature labeled figure caption is an artifact due to a change in filters during the experiment.

The Hall effect experiments showed that the deep levels pinning the Fermi level are donor-like defects and are present in concentrations of at least $1 \cdot 10^{15}$ cm^{-3}. No evidence for the presence of holes was detected indicating that the Fermi level is pinned in the upper half of the band gap in this material. This suggests that the positively charged carbon vacancy or carbon vacancy complexes located in the lower half of the band gap which were recently detected by EPR in s.i. 4H SiC material [9-11] are probably not responsible for compensation in our material. We suggest that the V_{Si}^{3-} defect is the dominant compensating deep level.

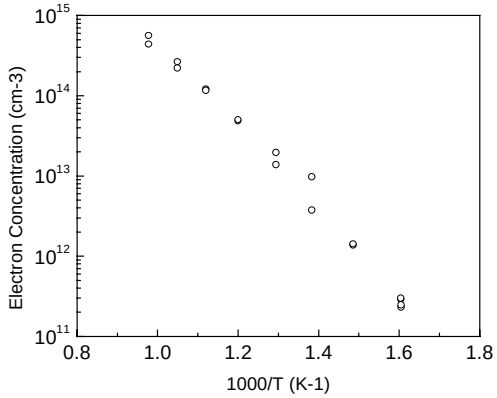

Fig. 2.4.5. Temperature dependent measurements of the n-type carrier concentration in HPSI 4H-SiC.

Fig. 2.4.5 shows the carrier concentration vs. inverse temperature for a sample from the same wafer as the sample used for the EPR experiments. The activation energy determined from the slope of the n vs 1/T data was 1.1 eV. All the Hall voltages were negative after averaging over both magnetic field direction and current direction. The carrier concentration and mobility were fitted to a two carrier model but the results indicated only one n-type carrier. This proves that the sample is n-type and that the Fermi level in the top half of the band gap. It is therefore most likely that

-

the defect or defects responsible for pinning the Fermi level in HPSI 4H-SiC are donor like. We also note that the carrier concentration at the highest measurement temperature was slightly under $1 \cdot 10^{15}$ cm^{-3}. This can be considered the minimum concentration of the compensating deep donor level and is in the range of the concentrations determined from EPR for the P defect. We have observed n-type conductivity in several HPSI samples as well as one s.i. HTCVD 4H SiC sample.

References:

1. Götz W., Schöner A., Pensl G., Suttrop W. Choyke W.J., Stein R., Leibenzeder S. Hall Effect and Infrared Absorption measurements on Nitrogen Donors in 4H-SiC // Mater. Science Forum - 1993.- 117-118. - P. 495 -500.
2. Mitchel W.C., Roth M.D., Evwaraye A.O., Yu P.W., Smith S.R. // Electronic Properties of Boron in p-type Bulk 6H-SiC // J. of Electronic Materials 1996. - 25. - N 5. - P. 863 - 867.
3. Kalabukhova E.N., Lukin S.N., Shanina B.D., Vodakov Yu.A., Lepneva A.A., Mokhov E.N. EPR in the 2-mm Range and Optical Absorption of the Native Defect in 4HSiC-Epilayers // Amorphous and Crystalline Silicon Carbide IY, "Springer Proceedings in Physics", 1992, V. 71, p. 703-707.
4. V.S. Vavilov, P.C. Euthymiou G.E. Zardas //Persistent photoconductivity in semiconducting III-V compounds// Uspekhi Fizicheskikh Nauk, 42 (2) 199-201 (1999)
5. E.N. Kalabukhova, S.N. Lukin, Yu.S. Gromovoy, E.N. Mokhov // EPR spectrum of donors in 6H SiC in a broad temperature range// Phys. Sol. St. Vol. 40, 1998, p. 1653 – 1657.
6. Schneider J., Müller H.D., Maier K., Wilkening W., Fuchs F. // Infrared spectra and electron spin resonance of vanadium deep level impurities in silicon carbide // Appl. Phys. Lett. - 1990. - 56. - P. 1184 - 1192.
7. Comprehensive ab initio study of properties of monovacancies and antisites in 4H SiC // L.Torpo, M. Marlo, T.E. M. Staab, R.M. Nieminen// J.Phys.: Condens. Matter 13, 6203-6231, 2001
8. A.Zywietz, J.Furthmuller, and F.Bechstedt //Vacancies in SiC: Influence of Jahn-Teller distortions, spin effects, and crystal structure // Phys. Rev. B, 59, 23, 15166- 15180, 1999.
9. N.T. Son, B. Magnusson, E. Janzen // Photoexcitation-electron-paramagnetic-resonance studies of the carbon vacancy in 4H SiC // Applied Physics Letters 81, 21, 3945-3947, 2002.
10. V.V. Konovalov, M.E. Zvanut, J.van Tol // 240 GHz electron paramagnetic resonance studies of intrinsic defects in as-grown 4H SiC// Phys. Rev. B Vol. 68 (2003) p. 012102 –(1 – 4).
11. W.E. Carlos, E.R. Glaser, B.V. Shanabrook // Optical and magnetic resonance signature of deep levels in semi-insulating 4H SiC// Proceedings of the ICDS22 (Physica B) accepted.
12. J.S. Blakemore, "Semiconductor Statistics" (Dover Publications, Inc. New York, 1987).

3.1, 3.2. Investigation of the spectral and the time characteristics of the photosensitive paramagnetic centers in s.-i. SiC, before and after annealing of the samples in the temperature interval from 1400^0 C to 1800^0 C.

The principle feature of s.-i. material is that the lifetime of the electrons and holes captured on the intrinsic defect and impurity levels is very long of about 10-14 hours and more at low temperature. The metastable state of the photosensitive intrinsic defects and impurities indicate that at low temperature the recombination rate of the photo-created carriers is very small. This phenomena is observed in many semiconductor structures and called persistent photoconductivity [4].

The recombination rates can be increased by raising the temperature or by illuminating the sample with photons of a below band gap wavelength.

A simple kinetics experiment was carried out to investigate the recombination process in the s. - i. 4H-SiC sample. Generally at least two photosensitive EPR signals are necessary to make such experiments possible. For this experiment, the EPR signals were first excited to a maximum value with above band–gap light then the exciting light was switched off and the quenching light is switched on. As was shown in Fig. 2 nitrogen and boron are not significantly populated prior to illumination (the intensity of boron EPR line in the dark is too small). Hence the first step in the experiment is to apply an excitation with UV light which induces the neutralization of the shallow donors and acceptors: $N^+ + B^- + e + h \rightarrow N^0 + B^0$. After the donors and acceptors have been neutralized, the effects of sub-band gap light can be studied. The spectral dependencies of the photo-quenching processes of the EPR spectra after excitation the sample with above band gap light is illustrated in Fig. 6**.** The nitrogen EPR spectrum is efficiently quenched after secondary illumination with below–band-gap light in the energy range of 3.0 eV to 2.2 eV and is completely eliminated for $h\nu \leq 2.20$ eV. A substantial quenching of the boron EPR spectra is also observed. The quenching band extends down to about 1.5 eV. The intensities of the boron EPR lines decay to about 0.25 of their excitation light–on value for $h\nu \leq 1.5$ eV. In addition, the I_P line with $g_{\|} = 2.0048$, $g_{\perp} = 2.0030$ appears at about 2.6 eV with maximum intensity at about 2.25 eV and persists in the EPR spectrum when the quenching light is turned off for more than 14 hours without a noticeable change in intensity.

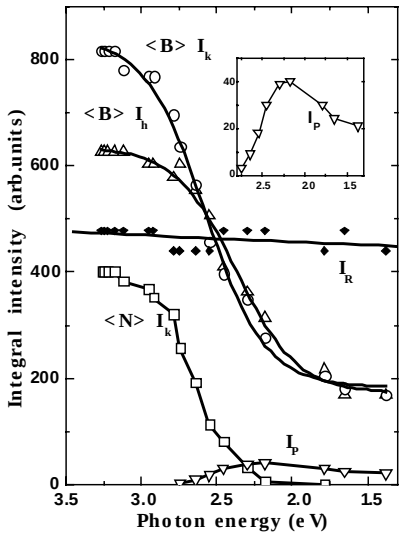

Fig. 3.1.1. The spectral dependencies of the photo – quenching processes after excitation of the unannealed semi - insulating 4H-SiC sample with above band gap light.

It should be noted that a comparison of the integral intensities of the boron and nitrogen EPR spectra, which are proportional to the concentrations of the paramagnetic centers shows the large difference between the amount of light–induced electrons (the concentration of nitrogen) and holes (the concentration of boron) in the s. - i. sample which was not annealed**.** This difference could be caused by existence of a large number of the structural defects in s. - i. material which also capture electrons. Indeed as was shown in Fig. 2.1.3, the 1400^0C heat treatment of the samples leads to increase of the light–induced electron amount captured by nitrogen and P center and as result the light-induced amplitudes of the donor and acceptor EPR signals become comparable.

The time dependence of the decay of the nitrogen resonance line for four different quenching photon energies is plotted in Fig. 3. This figure shows that a substantial enhancement of the recombination rate of the photo-created carriers starts at about $\Delta E_q = 2.36$ eV, which corresponds to the energetic distance of the deep donor level from the valence band: $E_g = \Delta E_q + \Delta E_{DL} \cong 2.36$ eV + 0.9 eV $\cong 3.26$ eV. Starting from 2.36 eV the number of the electrons released from nitrogen increase and hence the donor acceptor recombination process becomes more efficient. During quenching, the I_P line first appears when the intensity of the nitrogen EPR line decays to about 0.3 of its light–on value, independent of the energy of the quenching light. This indicates that the release of electrons from nitrogen is responsible for the appearance of the P center in the quenched EPR spectra.

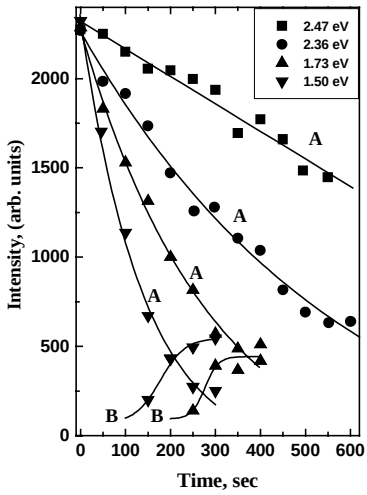

Fig.3. 1.3. Time dependence of the decay and rise of the nitrogen (A) and P center (B) EPR resonance lines for four different quenching photon energies.

The I_P line also appeared in the EPR spectrum after direct excitation with below band gap light as shown in Fig. 2c. When the below band-gap light was turned off, I_P and the boron lines persisted for more than 14 hours without a noticeable change in intensity, showing that no recombination processes occurred between the P center and boron. Subsequent illumination of the sample with UV light quenched the P center, restored the nitrogen EPR spectrum and enhanced the boron line to its maximum intensity, as seen in Fig. 2d**.** The rise and decay times of the intensity of the EPR signals of nitrogen, boron and the P center were found to depend on the intensity of the irradiating UV light. Under low intensity UV illumination the nitrogen and boron EPR lines increased slowly to their maximum values in approximately for 15 minutes while the I_P line completely vanished for this time, showing a correlation between the rise and decay of the EPR signals of nitrogen and the P center.

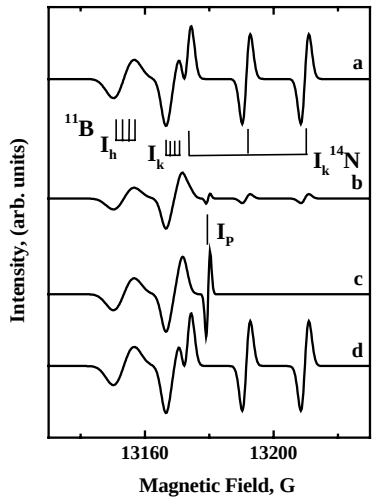

Fig.3.1.4. Photoresponse of EPR spectra in s.-i. 4H-SiC measured at 77 K and **B** ⊥ ***c***. a: UV light excitation, b: Spectra 21 hours after UV illumination, c: Visible light excitation, d: UV quenching of visible light induced signal.

The time characteristics of the photosensitive nitrogen paramagnetic center in F0847 s.-i. SiC have been investigated.

Fig. 3.1.5, 3.1.6 show the decay curves of the free carrier concentration captured by nitrogen and boron energy levels after excitation light is switched off. As was seen from Fig.1 b, 2, the fast component of decay curves of the carrier concentration captured by nitrogen and boron energy levels have a similar behavior and could be described by one exponent: exp(- 0.04 t)

Therefore it could be suggested that the fast component of decay curves is due to the recombination process between nitrogen and boron. Following the Shockley-Read-Hall (SRH) model, the electrons and holes can be successively captured by a single defect level and recombine.

The slow component of decay curves for nitrogen and boron have the different behavior and could be caused by the existence of trap level (P center) in the forbidden band. Electrons from nitrogen energy level recaptured by trap level where the lifetime of the trapped electrons is very long and recombination process between electrons captured by P center and holes captured by boron can be neglected which is supported by slow component for boron center.

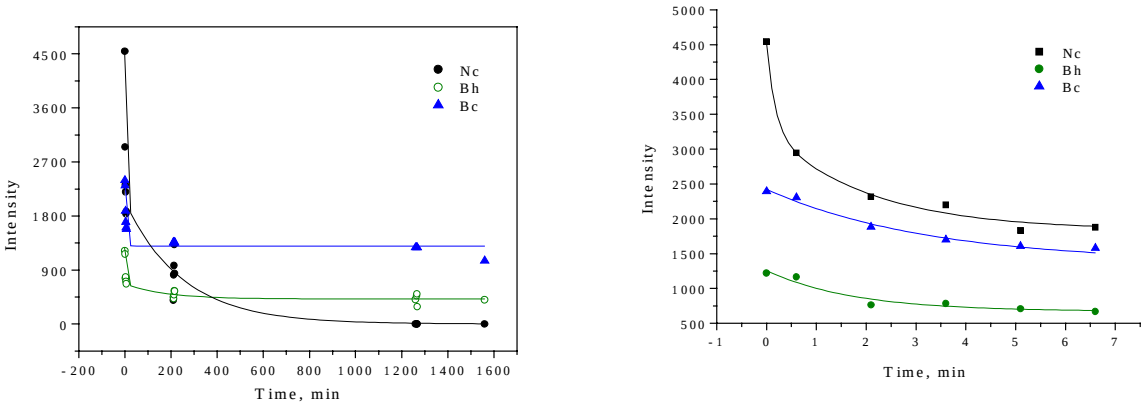

a **b**

Fig.3.1.5. Decay of nitrogen and boron EPR line intensity after UV excitation light (band gap) is switched off - **a**. Fast component of decay curve of the carrier concentration captured by nitrogen and boron energy levels - **b**. T = 77 K. Sample F0847

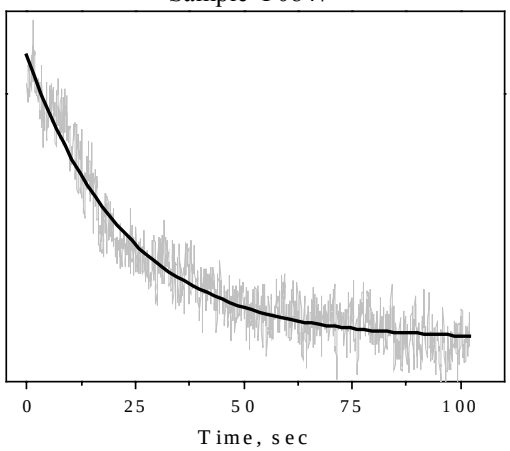

Fig. 3.1.6. Time dependence of the nitrogen EPR line intensity recorded after UV excitation light is switched off. Sample F0847. (Fast component). T = 77 K. Sample F0847

Fig.3.1.7. shows a sequential series of the light induced charge and discharge process for nitrogen with subsequent discharge in the dark. It is clear seen that the light induced charge and discharge process for nitrogen is well reproduced and the time discharge is smaller compare to that for nitrogen discharge in the dark.

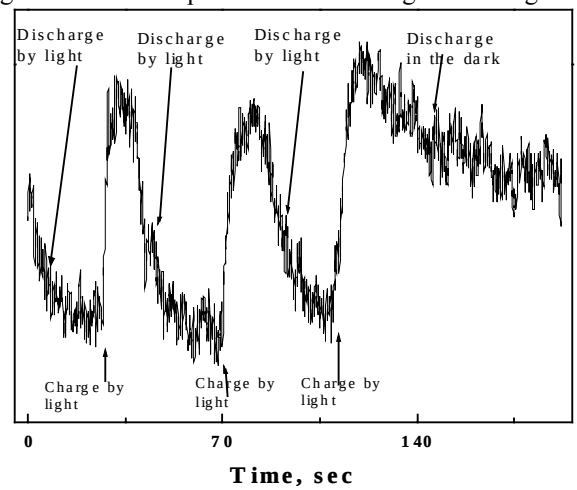

Fig.3.1.7. The charge and discharge process for nitrogen induced by light and nitrogen discharge curve recorded after UV excitation light is switched off. Sample F0847. T = 77K.

3.3. Analysis and processing of experimental EPR data. Comparison of the data obtained by EPR with that obtained by electrical and optical methods in AFRL/MLPS.

In accordance with the theoretical predictions made in [4,5] the possible model for the donor-like intrinsic defects located in the upper half of the band gap with the low spin state S =1/2 could be carbon and silicon vacancy in the negative charge state –1 and –3 respectively. As was seen from Table 1 similarity of the of the X center EPR parameters with E15 center associated with the carbon vacancy in the positive charge state +1 make it possible tentatively to assign the X center to the carbon vacancy in the negative charge state –1 whereas P center related to the silicon vacancy should be in the –3 charge state.

As result the photo quenching and photo excitation process of the donor-like intrinsic defects could be described by the following charge transitions:

$$V_C^- + e^- \rightarrow V_C^0;$$
$$V_{Si}^{2-} + e^- \rightarrow V_{Si}^{3-}.$$

Following the theoretical prediction the high spin configuration S = 1 is more preferably for the V_{Si}^{2-} than S = 0. The fact that the EPR spectrum with S = 1 was not found in HPSI 4H SiC could be explained either by the location of the Fermi level in HPSI 4H SiC above the energy level of the V_{Si}^{2-} with S = 1 in the dark or its other spin configuration S =0.

Thus, there are five photosensitive paramagnetic centers which can be activated in a paramagnetic state by excitation with light. Two of them are the well known nitrogen and boron contaminating impurities which are not populated prior to illumination. The illumination of the sample by above band gap (UV) light, as shown in figure 3.3.1, induces the neutralization of the shallow donors and acceptors:

$$N^+ + B^- + e + h \rightarrow N^0 + B^0$$

and as result the EPR spectra of nitrogen and boron are observed simultaneously in the EPR spectrum.

The excitation and quenching of the EPR spectrum of the s. - i. 4H-SiC sample may be explained by the electronic processes given in Fig.3.3.1. The energy gap of 4H-SiC is assumed to be 3.26 eV. Transition (1) corresponds to the excitation process when electrons excited from the valence band into the conduction band with the subsequent capture of the electrons from the conduction band by donor centers including nitrogen, ND1, P, X center depending on the position of the quasi Fermi level and the holes from the valence band by boron causing the corresponding EPR signals of nitrogen (ND1, P center) and boron.

Photoconductivity is observed for this process.

$$N^+ + B^- + e + h \rightarrow N^0 + B^0;$$
$$C_{Si}^0 + N^+ + B^- + e + h \rightarrow N^0 + C_{Si}^- + B^0$$
$$V_{Si}^{2-} + B^- + e + h \rightarrow V_{Si}^{3-} + + B^0$$

The transition of the donor impurities and defects from the diamagnetic to the paramagnetic state could also be induced indirectly by excitation of an electron from the valence band to an ionized donor

$$N^+ + C_{Si}^0 + h\nu \rightarrow N^0 + C_{Si}^- + h_{VB} \text{ (transition 2, 3)}$$

followed by capture of the hole by boron. .

Photo quenching process for the P and X (transition 4) defect could be described by the following charge transitions

$$V_C^- + h\nu \rightarrow V_C^0 + e_{CB}$$
$$V_{Si}^{3-} + h\nu \rightarrow V_{Si}^{2-} + e_{CB}$$

The experimental data obtained above are shown that the transition of the donor P center from diamagnetic to the paramagnetic state could be induced indirectly by excitation of an electron from the valence band to an ionized donor,

$$P^{2-} + h\nu \rightarrow P^{3-} + h_{VB} \text{ (see transition 2),}$$

followed by capture of the hole by boron, or, alternatively, the excitation of an electron from X center to the conduction band,

$$X^- + h\nu \rightarrow X^0 + e_{CB} \text{ (see transition 4),}$$

with subsequent capture of electrons from the conduction band by P center.

Transition (5) is the donor acceptor recombination process involving the photo-induced deep donor center P. The correlation observed between the decay and rise in intensity of EPR signal of nitrogen and P center indicates that there is a intercenter charge transfer process between shallow nitrogen and deep donor center. The efficiency of this process

in SiC is independent from the concentration of nitrogen but promoted by increasing the concentration of deep donor center and by lowering the Fermi level to the midgap.

It should be noted that the lifetime of electrons trapped on the P center is very long, 15 - 20 hours after the photo-excitation was terminated. Hence the P deep donor center could be involved in the TR process as the possible life-time controlling defect for the low temperature TR process in s. - i. 4H-SiC.

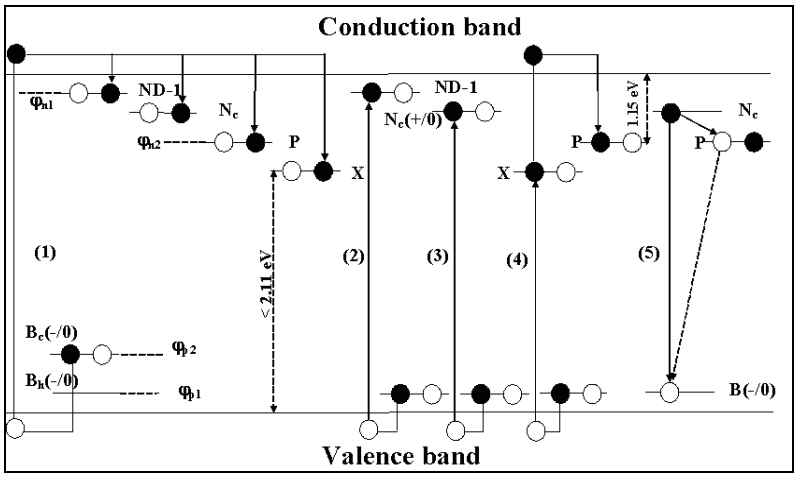

Figure 3.3.1 Simple scheme - model for the electronic transitions in s.-i. 4H SiC sample.

Table 3.3.1. Parameters of EPR spectra of X, P and ND1 center observed in HPSI 4H SiC and E15 EPR spectrum observed in irradiated p-type 4H SiC [6].

Center	$g_{\parallel}$	$g_{\perp}$	Symmetry	ΔT, K	Spin	Charge	Model	$E_V + E_i$, eV	
								Experiment	Theory [4, 5]
E15	2.0032	2.0048	C_{3V}	25 - 140	1/2/0	1+/0	V_C^+	1.47	h: 1.53 c: 1.41
X_h	2.0025	2.0044	C_{3V}	25 - 100	0/1/2	0/1–	V_C^-	2.11	h: 1.90
X_c	2.0028	2.0043	C_{3V}	25 - 100	0/1/2	0/1–	V_C^-	2.11	c: 2.09
X_c			C_{1h}	4.2-40	0/1/2	0/1–	V_C^-	2.11	c: 2.09
P_h	2.0048	2.0030	C_{3V}	50 - 77	0/1/2	2–/3–	V_{Si}^{3-}	2.11	h: 2.26
P_c	2.00365	2.00365	T_d	50 - 77	0/1/2	2–/3–	V_{Si}^{3-}	2.11	c: 2.14
$ND1_h$	2.0063	2.0006	C_{3V}	4.2-50	0/1/2	0/1–	C_{Si}^-	3.19	
$ND1_C$	2.0058	2.0033	C_{3V}	4.2-50	0/1/2	0/1–	C_{Si}^-	3.19	

The excitation and quenching spectra of the nitrogen and boron EPR signals may be explained by a recombination process between nitrogen and boron that involves the P center.

The excitation and quenching EPR spectra can be understood as due to two competing processes. One is the recombination process between nitrogen and boron and second is the charge transfer process occurring between shallow nitrogen and deep donor –like P center resulting in the appearance and subsequent disappearance of I_P EPR line in the quenched EPR spectra. As was shown in Ref. [5] the efficiency of the intercenter charge transfer process in SiC is enhanced by increasing the concentration of deep donors and by lowering the Fermi level to midgap after which the nitrogen donors tends to interact less with the conduction band and more with states below them.

It should be noted that the lifetime of electrons trapped on the P center is very long, 15 - 20 hours. Taking into account that the boron lines also persist in the quenched EPR spectrum, it can be concluded that recombination between nonequilibrium carriers is impeded by the presence of the P center. Thus the P center is strongly involved in the trapping and recombination (TR) process and is possibly the dominant life-time controlling defect at low temperature in these samples.

The analysis of time characteristics of carrier concentration captured by nitrogen energy level after excitation light is switched off has been performed. The two components of decay in carrier concentration could be described by kinetic equations written for a single recombination center, nitrogen level and trap level responsible for the carrier concentration decay curve.

Below are the equations written for general case without consideration of the model describing the experimental data. The electron population in the trap m and nitrogen n_d level, carrier concentration in the conduction (n), valence band (p) and recombination level r is governed by

$$\begin{aligned} dm/dt &= \gamma_n n(M-m) - \gamma_n m N_{cM} - \gamma_p mp \\ &\quad + \text{e-capture} - \text{e-emisson} - \text{h-capture} \\ dn/dt &= k\beta I - \gamma_n rn - \gamma_n n(M-m) + \gamma_n m N_{cM} \\ &\quad - \text{e-capture} - \text{e-capture} + \text{e-emisson} \\ dr/dt &= \gamma_n rn + \gamma_p(R-r)p - \gamma_n r N_{cR} \\ &\quad - \text{e-capture} + \text{h-capture} - \text{e-emisson} \\ dp/dt &= k\beta I - \gamma_p(R-r)p + r\gamma_n N_{cR} - \gamma_p mp \\ &\quad - \text{h-capture} + \text{h-emisson} - \text{h-capture} \\ dn_d/dt &= \gamma_n n(N_d-n_d) - \gamma_n n_d N_{cM} - \gamma_p mp \end{aligned}$$

where γ_n (γ_p) = σ_n (σ_p) ν_{th}; σ_n (σ_p) is the capture cross section for electrons (holes), ν_{th} the thermal velocity of carriers; M - trap concentration; R – concentration of the recombination center; N_d - nitrogen concentration, n and p are the carrier concentration

$$N_{cM} = N_c\exp(-E_t)/kT); \; N_{cR} = N_c\exp(-E_r)/kT);$$

where k is the Boltzmann constant, N_c, – the effective density of states in the conduction band, T the temperature
β - quantum yield for pair number; k – absorption factor of the light; I – Intensity of the light.

1. We can consider a simplified case assuming that the thermal emissions can be neglected at low temperature T = 77 K.

$$\begin{aligned} dm/dt &= \gamma_n n(M-m) - \gamma_p mp - T_{12}m(N_d-n_d) + T_{21}n_d(M-m) \\ &\quad + \text{e-capture} - \text{h-capture} \\ dn_d/dt &= \gamma_n n(N_d-n_d) - \gamma_p mp + T_{12}m(N_d-n_d) - T_{21}n_d(M-m) \\ dr/dt &= \gamma_n rn + \gamma_p(R-r)p \\ &\quad - \text{e-capture} + \text{h-capture} \end{aligned}$$

2. Considering the charge transfer process between nitrogen (1) and trap level (2) the terms $T_{12}m(N_d-n_d)$ and $T_{21}n_d(M-m)$ should be added to the rate equations to describe the evolution of the filling of the nitrogen and trap centers due to its charge transfer.

There are several unknown parameters in the equations and it is necessary to set their values to decide this equations. The initial excess carrier concentration could be set $1x10^{16}cm^{-3}$ as expected from the excitation intensity in most cases. All capture cross sections of the recombination center are initially assumed to be $1x10^{15}cm^2$, which is a typical value for levels without capture barriers, and electron capture cross section of the trap σ_m could be varied.
The trap level E_c-E_t is fixed at 1.15eV. The concentration of the trap is fixed at $2x10^{16}cm^{-3}$.
Further consideration of the model and equations is in progress to describe the trapping recombination process observed in s.-i. samples.

4.1. 4.2. Investigations of the temperature characteristics of the photosensitive paramagnetic centers in s.-i. SiC crystals in the temperature interval from 77 K to 4.2 K before and after annealing.

The investigations of the temperature characteristics of the X center in DC0184 -17 s.-i. SiC crystals in the temperature interval from 77 K to 4.2 K has been performed.

Fig. 4.1.1 shows EPR spectrum of X defect recorded at $\mathbf{B_0} \parallel \mathbf{c}$. At T =77 K EPR spectrum consists of two single lines with axial symmetric g-factors corresponding to the two inequiavalent positions residing by defect center. When the temperature decrease the transformation of one single line X_c into four EPR lines is occured showing that the symmetry of EPR spectrum is changed from axial C_{3v} to monoclinic symmetry for the defect residing cubic site.

The behavior of the X defect EPR spectrum is typically for the center with Jahn-Teller distortion when degeneracy of three nearest neighbours C (Si) of the defect about c-axis at low temperature could be removed by Jahn-Teller distortion.

According to the single one-electron model, the electronic structure of a vacancy in a covalent solid is described by molecular orbitals constructed from four dangling bonds next to the vacancy. The defect molecular orbitals consist of the lowest a_1 one and a triply degenerate t_2 one, so a_1 can accommodate two electrons and t_2 six.

However, the crystal can usually gain energy by relaxing atoms next to the vacancy. Lowering the symmetry destroys the degeneracy of the t_2 orbital, provided that the energy gained by the overlapping dangling bonds overcomes the energy lost in distorting the lattice. This effect is called the Jahn-Teller distortion.

For a vacancy system, which is not subject to a the Jahn-Teller distortion, the exchange interactions can result in high-spin ground states. In fact, for Si vacancy in SiC the high spin ground state is more prefarably. As follows from theoretical prediction Si vacancy is generally T_d symmetry or close to that, less frequently a lower symmetry like $C_{3v.}$

On the other hand carbon vacancies in neutral or negative charge states are characterized by large Jahn-Teller distortion inward relaxations, resulting in breaking of the T_d symmetry towards D_{2d} symmetry. In addition for the singly negative charge state it was found a significant difference between C vacancies at cubic and hexagonal lattice.

To explain the observed temperature transformation of EPR spectrum of X defect let us suppose that X defect has one unpaired electron. In this case the neutral state of the X defect has seven electrons and the ground state for undistorted tetrahedron $Si(C_4)$ or $C(Si_4)$ is threefold degenerate of T symmetry. For the defect residing the hexagonal site the unpaired electron is localized at the orbital parallel to the c axis and symmetry of the EPR spectrum does not change with increasing the temperature. For the defect residing the quasicubic site the unpaired spin occupies one of three others orbital perpendicular to the c axis at low temperature and the symmetry of the defect is low. At elevated temperature due to the thermally activated reorientation of the electron between three bonds about c-axis the symmetry of the defect EPR spectrum residing cubic site becomes higher (C_{3v}).

Further investigation of X center EPR spectrum at high frequency (140 GHz) in progress.

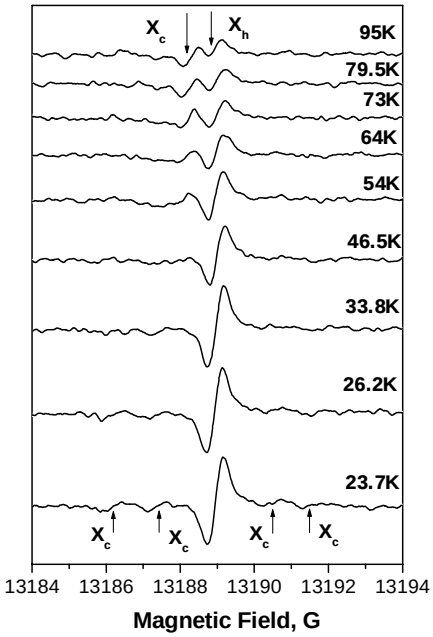

Fig. 4.1.1. Temperature transformation of X defect EPR spectrum.

The temperature characteristics of the photosensitive paramagnetic centers in DC0184 -17 (D-23) and (D4) F0847 after annealing of the samples up to 1800 C have been studied.

Considering that the energy levels of the defect responsible for s.-i. feature of the samples are localized in the midgap the temperature interval for the investigation of the photosensitive paramagnetic centers has been selected from 77 K to 140 K.

Fig. 4.1.2 shows the temperature evolution of EPR spectrum observed in DC0184 -17 (D-23) sample in the dark which was preliminary illuminated by UV light. After illumination of the sample with UV light the EPR spectrum consists of boron and P center EPR lines the intensities of which were not changed after 48h exposition in the dark.

As temperature rises EPR line of boron residing hexagonal site disappeared at T = 98 K while intensity of EPR lines of boron residing quasicubic site and P center were decreased and disappeared at T = 107 K. When the sample is cooled down a new line labeled L with ΔH_L= 1.65 Gs appeared in EPR spectrum at 86 K The g-factor of L defect EPR line coincides with that of cubic boron EPR line but their line width differs from each other: ΔH_L= 1.65 Gs, ΔH_B = 3.37 Gs. The further cooling of the sample up to 77 K gave rise to the appearance of cubic boron EPR line which becomes apparent due to the broadening of the EPR signal up to ΔH = 3.79Gs. The subsequent rising of the temperature up to 140 K gave rise to the ionization of free carriers from L defect and boron energy level and as result EPR lines of boron and L defect were disappeared. When the temperature goes down EPR line of X defect appeared in EPR spectrum which can be easy recognized by its small width line: ΔH_X = 1.26 Gs.

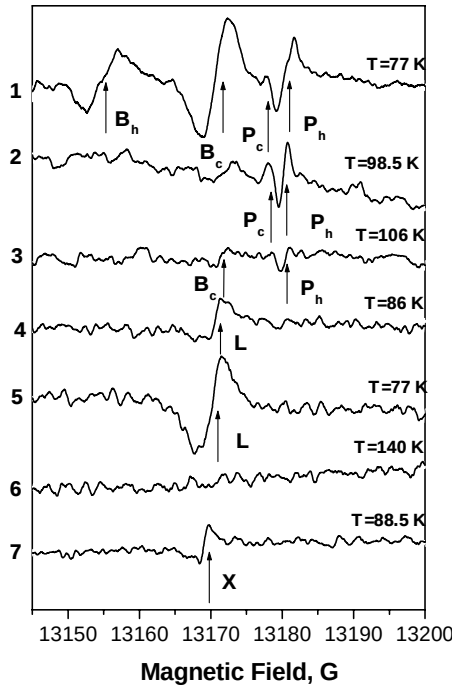

Fig. 4.1.2 The temperature evolution of EPR spectrum in DC0184 -17 (D-23) sample in the dark preliminary excited by UV light. 1- 48 h after the light is switched off.

The same temperature characteristics have been studied in (D4) F0847 s.-i. sample in which the position of the Fermi level differs from that in DC0184 -17 (D-23) sample. As was seen from Fig. 4.1.3, EPR spectrum of boron and nitrogen appeared in EPR spectrum after illumination of D4 F0847 s.-i. sample with UV light. Nitrogen EPR spectrum practically vanished in EPR spectrum after 26 h exposure in the dark.

Fig. 4.1.4 shows the temperature evolution of EPR spectrum observed in (D4) F0847 s.-i. sample preliminary illuminated by UV light and afterwards keeping 26 h in the dark.

After the first stage of the heating up to 102 K EPR spectrum of boron disappears and simultaneously EPR spectrum of P defect is appeared in EPR spectrum.

The second stage of the heating up to 113 K leads to ionization of the carriers both from boron and P defect energy levels and as a result their EPR spectra are vanished at 113 K. The free electrons are recaptured by L defect and when the temperature is lowered EPR line from L defect appears in EPR spectrum. After second stage of the heating up to 145 K the free electrons are recaptured by X defect and EPR line of X defect is observed in EPR spectrum when the temperature goes down.

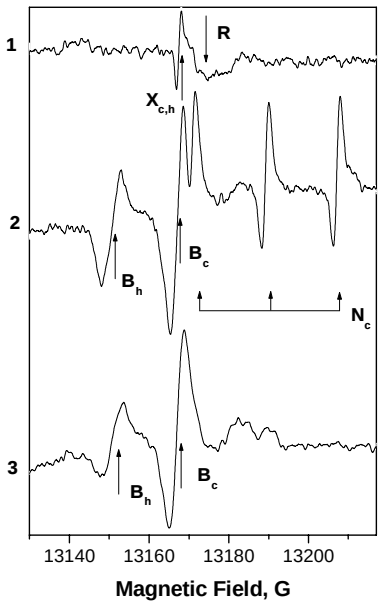

Fig. 4.1.3. Photoresponse of EPR spectra in (D4) F0847 s.-i. sample measured at 37 GHz and 77 K. 1 – dark; 2 – illumination with UV light; 3 - 26 h after the light is switched off. $\mathbf{B_0} \perp \mathbf{c}$. B_c, B_h -EPR spectrum of boron ^{11}B, N_c - EPR spectrum of nitrogen.

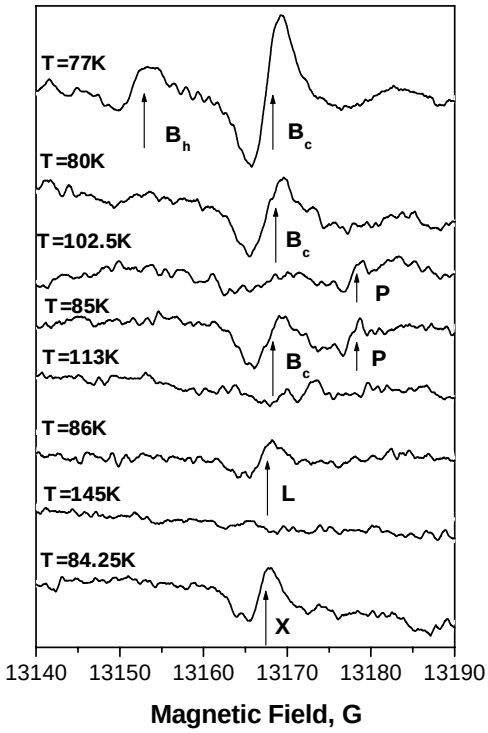

Fig. 4.1.4. The temperature evolution of EPR spectrum spectra in (D4) F0847 s.-i. sample in the dark preliminary excited by UV light. 1- 26 h after the UV light is switched off.

4.3. Analysis and processing of experimental data. The comparison of the data obtained by EPR with that obtained by electrical and optical methods.

The temperature evolution of the EPR spectrum observed in s.-i. sample indicates that at elevated temperature non-equilibrium electrons are released from P center energy level due to the moving of the Fermi level down to the midgap with increasing the temperature. The free electrons are captured by the level at which the Fermi level is locked at given temperature. First stage of the heating up to 107 K locks the Fermi level at L defect level while the second stage of the heating up to 140 K locks the Fermi level at X defect level. As result EPR spectrum of L defect appeared after first stage of the heating and X defect appeared after second stage of the heating in EPR spectrum of s.-i. sample. The Fig. 4.1.5 shows the electron recapture process between three levels with the difference in energy of

$$\Delta T = 140\ K - 107\ K = 33\ K = 2.85\ meV$$

After first stage of the sample heating up to 107 K the non-equilibrium holes are also released from boron energy level and again are recaptured by boron energy level when the temperature goes down. As result the EPR signal from cubic boron is restored in EPR spectrum. After second stage of the heating the boron EPR line is not appeared in EPR spectrum showing that the holes released from boron energy level are recaptured by other nonparamagnetic energy level. The temperature of around 100 K = 8 meV is too low for the ionization of the free holes from boron energy level with ionization energy of E_i = 0.35eV into the valence band.

The same free carrier recapture process is observed in s.-i. sample with other location of the Fermi level. In this case the electrons are released from nitrogen energy level and subsequent recaptured by a series closely located energy levels of P, L and X defects.

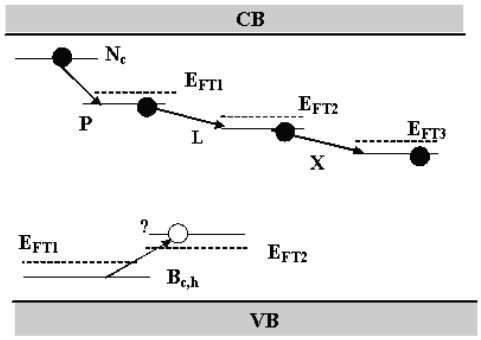

Fig. 4.1.5. Temperature induced charge transfer process in 4H SiC s.-i. material.

The intercenter charge transfer process is shown to represent an important shunt for the carrier recombination process in high purity semi-insulating 4H SiC material. The following electronic model for trapping recombination process in s.-i 4H SiC is proposed and given in Fig. 4.1.6. The energy gap of 4H-SiC is assumed to be 3.26 eV.

Transition (1) corresponds to the excitation of the sample by band gap light when electrons excited from the valence band into the conduction band with the subsequent capture of them by nitrogen, ND1, P defects, depending from the temperature and location of the quasi Fermi level, and the holes from the valence band by boron. Photoconductivity is observed for this process.

Transition (2, 3) corresponds to the excitation of the sample by below-band-gap light. When the photon energy corresponds to the energetic distance of the nitrogen or ND1 defect from the valence band, the electrons excited from valence band are captured on the energy level of nitrogen, ND1 defect and holes from the valence band by boron.

Transition (4) corresponds to the excitation of the sample by below-band-gap light When the photon energy corresponds to the energetic distance of the X center from the valence band, the electrons excited from the X center are captured on the energy level of the P center via the conduction band and holes from the valence band by boron. The correlation observed between the rise and decay in intensity of the P and X defect EPR signals under photo excitation could be explained by charge transfer process between two intrinsic defects.

Transition (5) is the donor acceptor recombination process between nitrogen and boron involving the deep donor-like P defect as the life-time controlling defect for the low temperature recombination process in s. - i. 4H-SiC.

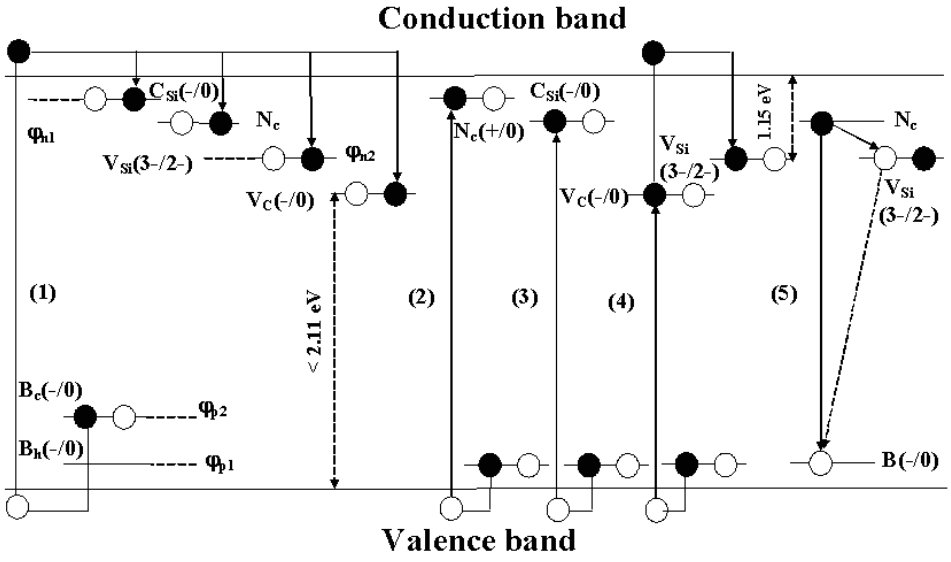

Fig. 4.1.6. Simple electronic model for trapping recombination process occurring in s.-i. 4H SiC samples.

Conclusion.

Thus, it was established that in all HPSI 4H SiC samples under investigation Fermi level was pinned at X defect level located in the upper half of the band gap in the dark. All others impurities and defects such as nitrogen, boron and P defect related to the isolated silicon vacancy are in a non-EPR active state. Excitation of the samples with the light gives rise to the transition of them from a diamagnetic ground state into observable paramagnetic state depending from the location of the quasi Fermi level at given temperature. The investigation of the photo excitation and quenching of the EPR spectrum in the HPSI 4H SiC samples shows that the energy level of the P defect is also located in the upper half of the band gap approximately at 1.15 ± 0.06eV below E_C.

The EPR data obtained are confirmed by temperature dependent Hall effect measurements. The Hall effect experiments proves that the sample is n-type and the deep levels pinning the Fermi level are donor-like defects which are present in concentrations of at least $1 \cdot 10^{15}$ cm^{-3}. This can be considered the minimum concentration of the compensating deep donor level and is in the range of the concentrations determined from EPR for the P defect. No evidence for the presence of holes was detected indicating that the Fermi level is pinned in the upper half of the band gap in this material. This suggests that the positively charged carbon vacancy or carbon vacancy complexes located in the lower half of the band gap which were recently detected by EPR in s.i. 4H SiC material are probably not responsible for compensation in our material. The V_{Si}^{3-} defect is suggested to be the dominant compensating deep level.

On the base of the direct observation of the temperature induced intercenter charge transfer process occurring in the high purity semi-insulating HPSI 4H SiC material by photo EPR method it was established that intercenter charge transfer process between a series of deep donor like defects is to be efficient when quasi Fermi level is moving towards the middle of the band gap with increasing the temperature.